

Recent advances in oomycete genomics

Jamie McGowan^{a,b}, David A. Fitzpatrick^{a,b,*}

^aGenome Evolution Laboratory, Department of Biology, Maynooth University, Maynooth, County Kildare, Ireland

^bKathleen Lonsdale Institute for Human Health Research, Maynooth University, Maynooth, County Kildare, Ireland

*Corresponding author: e-mail address: david.fitzpatrick@mu.ie

Contents

1. The oomycetes	2
2. Oomycete genomes	6
3. Oomycete phylogenomics	16
4. Oomycete mitochondrial genomes	20
5. The impact of horizontal gene transfer on oomycete evolution	22
6. Genome mining for oomycete effectors	25
6.1 Apoplastic effectors	26
6.2 Cytoplasmic effectors	28
7. Oomycete OMICS studies	32
7.1 Oomycete proteomics studies	32
7.2 Oomycete transcriptomics studies	35
8. Tools for oomycete genomics	38
9. Oomycetes in the post-genomic era	40
10. Conclusions and future outlook	43
Acknowledgments	44
References	44

Abstract

The oomycetes are a class of ubiquitous, filamentous microorganisms that include some of the biggest threats to global food security and natural ecosystems. Within the oomycete class are highly diverse species that infect a broad range of animals and plants. Some of the most destructive plant pathogens are oomycetes, such as *Phytophthora infestans*, the agent of potato late blight and the cause of the Irish famine. Recent years have seen a dramatic increase in the number of sequenced oomycete genomes. Here we review the latest developments in oomycete genomics and some of the important insights that have been gained. Coupled with proteomic and transcriptomic analyses, oomycete genome sequences have revealed tremendous insights into oomycete biology, evolution, genome organization, mechanisms of infection, and metabolism. We also present an updated phylogeny of the oomycete class using a phylogenomic approach based on the 65 oomycete genomes that are currently available.

1. The oomycetes

Oomycetes are filamentous, microbial eukaryotes that morphologically resemble fungi (Beakes, Glockling, & Sekimoto, 2012), but belong to the species-rich group of stramenopiles (Burki, Roger, Brown, & Simpson, 2019), which contains other diverse organisms such as diatoms and brown algae (Fig. 1). Oomycete species are highly diverse in terms of their lifestyles, pathogenicity and host ranges. More than 60% of known oomycete species are pathogens of plants (Thines & Kamoun, 2010). Together, they represent one of the biggest threats to global food security and natural ecosystems. Most notorious among oomycete species is *Phytophthora infestans*, a hemibiotrophic pathogen that causes late blight of tomato and potato (Haas et al., 2009), and was the causative agent of the Irish potato famine which resulted in the death of one million people and the displacement of another million. *Phytophthora sojae* is another highly destructive species that causes billions of dollars worth of soybean crop loss each year (Tyler, 2007). *Ph. infestans* and *Ph. sojae* are examples of species with narrow host ranges. In contrast, *Phytophthora ramorum*, the “sudden oak death” pathogen, has a wide host range that can infect more than 100 host species (Rizzo, Garbelotto, & Hansen, 2005). *Phytophthora cinnamomi* has a very wide host range and is thought to be able to infect more than 3000 host species (Hardham, 2005). Virtually all dicotyledon plants are

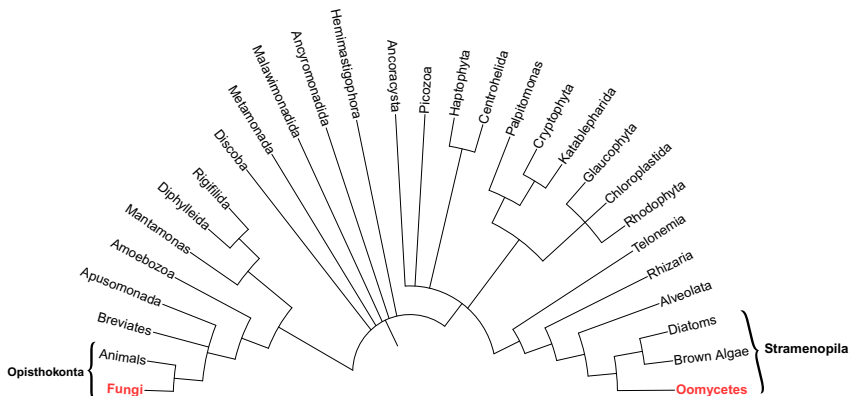


Fig. 1 Simplified phylogeny of the eukaryotes showing the distant relationship between oomycetes and fungi. Adapted from Burki, F., Roger, A. J., Brown, M. W., & Simpson, A. G. B. (2019). The new tree of eukaryotes. *Trends in Ecology & Evolution*, 35, 1–13. <https://doi.org/10.1016/j.tree.2019.08.008>.

susceptible to infection by one or more *Phytophthora* species (Kamoun, 2003). Other economically devastating oomycete species include the obligate biotrophic downy mildews, *Bremia lactucae* and *Plasmopara viticola*, some of the most important pathogens of lettuce and grapevine, respectively (Dussert et al., 2019; Fletcher et al., 2019).

While the majority of attention is typically placed on plant pathogenic oomycetes, many oomycete species cause infections in other economically and ecologically important organisms. For example, *Saprolegnia* species are pathogens of amphibians, crustaceans, fish, and insects (Jiang et al., 2013). In particular, *Saprolegnia parasitica* is a freshwater fish pathogen that is predominant in farmed salmon populations, resulting in losses of more than 10% (van den Berg, McLaggan, Diéguez-Urbeondo, & van West, 2013). *Pythium oligandrum* and *Pythium periplocum* are pathogens of fungi and oomycetes, acting as powerful biocontrol agents that can combat plant pathogenic fungi and oomycetes (Benhamou et al., 2012; Kushwaha, Vetukuri, & Grenville-Briggs, 2017b). *Pythium guiyangense* is a highly virulent pathogen of mosquitos and is a potential biocontrol agent to efficiently manage mosquito populations (Shen et al., 2019). Some oomycete species, such as *Pythium insidiosum*, can cause fatal infections in humans and other mammals typically resulting in amputations or even death (Gaastra et al., 2010).

The oomycete class is divided into four “crown” orders—the Peronosporales, Pythiales, Albuginales, and Saprolegniales (Fig. 2). The Peronosporales order is the best studied order and includes the phytopathogenic *Phytophthora*, *Nothophytophthora* and *Phytopyrium* genera as well as the downy mildew *Bremia*, *Hyaloperonospora*, *Peronospora*, *Plasmopara*, *Pseudoperonospora* and *Sclerospora* genera (Fletcher et al., 2019; McCarthy & Fitzpatrick, 2017). The Pythiales order includes the *Pythium* genus and *Pilasporangium* (Fig. 2) (Adhikari et al., 2013). Within this order are a mix of animal, fungal, plant and oomycete pathogens. The Albuginales order includes the plant-parasitic *Albugo* genus (Fig. 2) which causes “white blister rust” on many valuable crop species (Kemen et al., 2011; Links et al., 2011). The Saprolegniales order is the most basal of the four crown orders (Fig. 2) and includes animal and plant pathogens. Genera belonging to the Saprolegniales order include *Achlya*, *Aphanomyces*, *Saprolegnia* and *Thraustotheca* (Misner, Blouin, Leonard, Richards, & Lane, 2015).

Oomycetes were previously thought to be fungi due to similar morphological characteristics, filamentous growth, osmotrophic uptake of nutrients and similar ecological roles (Leonard et al., 2018; Richards, Dacks,



Fig. 2 Maximum-likelihood phylogeny of the 65 oomycete species based on the concatenation of 102 conserved BUSCO sequences. The stramenopile *Hyphochytrium catenoides* is included as an outgroup. All nodes have 100% bootstrap support except where indicated. Species are colored according to order. *Phytophthora* clades are indicated as designated by Blair, Coffey, Park, Geiser, and Kang (2008) and *Pythium* clades are as designated by de Cock et al. (2015).

Table 1 Typical features that differ between oomycetes and fungi.

Character	Oomycetes	True fungi
Neighboring taxonomic groups	Diatoms and brown algae	Animals
Hyphal structure	Aseptate and multinucleate	Single cells or septate hyphae, with one or more nuclei per compartment
Ploidy of vegetative hyphae	Diploid	Typically haploid or dikaryotic
Cell wall composition	Cellulose and β -1,3 and β -1,6 glucans	Chitin and β -1,3 and β -1,6 glucans
Pigmentation	Usually unpigmented	Hyphae and/or spores are commonly pigmented
Secondary metabolites	None described	Common
Motile asexual spores	Biflagellated zoospores	Rare but some exceptions such as chytrids
Sexual spores	Oospores	Various types

Adapted from Judelson, H. S., & Blanco, F. A. (2005). The spores of *Phytophthora*: Weapons of the plant destroyer. *Nature Reviews Microbiology*, 3(1), 47–58. <https://doi.org/10.1038/nrmicro1064>.

Jenkinson, Thornton, & Talbot, 2006). Even today, oomycetes are commonly mistakenly referred to as fungi. Several key differences distinguish oomycetes (pseudo-fungi) from “true-fungi,” some of which are summarized in Table 1. Phylogenetically, fungi branch with animals within the Opisthokonta (Fig. 1), whereas the oomycetes are stramenopiles within the SAR (Stramenopila, Alveolata, and Rhizaria) supergroup placing them more closely related to brown algae and diatoms (Fig. 1) (Burki et al., 2019).

Oomycetes cause infection by secreting large arsenals of effector proteins that breakdown host cell components, modulate host immune responses and trigger host necrosis (Kamoun, 2006; McGowan & Fitzpatrick, 2017). Effector families can be divided into two broad categories based on where they localize—apoplastic effectors that act outside the host cell and cytoplasmic effectors that enter the host cell (Wawra et al., 2012). Apoplastic effectors families include large families of hydrolytic enzymes such as glycoside hydrolases and proteases, as well as toxins including the necrosis-inducing proteins (NLPs) and phytotoxic protein family (PcF) proteins. Cytoplasmic oomycete effectors include the RxLR and Crinkler

(CRN) family of effectors, which contain conserved translocation motifs that facilitate their delivery inside host cells (Haas et al., 2009; Tyler et al., 2006).

In recent years, in line with advancements in next-generation sequencing technologies, there has been an increased pace of oomycete genome sequencing. At the time of writing, 65 oomycete species (Table 2) have publicly available genome sequences deposited in databases such as the NCBI GenBank (Benson et al., 2012). Such genome sequencing projects have yielded tremendous insights into oomycete biology, evolution, effector arsenals, genome organization, metabolism and mechanisms of infection. Here we review recent developments in oomycete genomics and highlight some of the important findings that have been reported.



2. Oomycete genomes

In 2006, the first oomycete genome sequences were published for *Ph. ramorum* and *Ph. sojae* (Tyler et al., 2006). Whole-genome shotgun sequencing produced a ninefold coverage assembly of the 95 Mb *Ph. sojae* genome and a sevenfold coverage assembly of the 65 Mb *Ph. ramorum* genome (Table 2). Comparative genomic analysis identified rapid expansion/loss and diversification of secreted protein families associated with pathogenicity, including glycoside hydrolases, proteases and effector families such as elicitors, NLPs and the cytoplasmic RxLR and CRN families (Jiang, Tyler, & Govers, 2006; Jiang, Tyler, Whisson, Hardham, & Govers, 2006; Tyler et al., 2006). These analyses showed that the secretome of both species has undergone rapid diversification and is evolving at a faster rate than the overall proteome, as 11% and 17% of the secreted proteins were found to be unique to *Ph. ramorum* and *Ph. sojae*, respectively, compared to 4% and 9% of the overall proteomes of each species, respectively. Large multigene families in each species were also reported. The genome sequences show extensive collinearity/synteny of orthologs between the two species, with over 75% of exons aligning in a whole-genome alignment (Tyler et al., 2006).

The *Ph. infestans* genome was published in 2009, revealing a much larger genome assembly size of 229 Mb (Table 2) and extremely high repeat content comprising 74% of the genome assembly, compared to 28% and 13% in *Ph. sojae* and *Ph. ramorum*, respectively (Haas et al., 2009). The *Ph. infestans* genome also contains large expansions of effector proteins, in particular ~60% more putative RxLR effectors were identified in *Ph. infestans* than

Table 2 List of the 65 oomycete genome assemblies that are available at the time of writing.

Species	Clade ^a	Order	Host	Genome Size Mb ^b	Reference ^c
<i>Albugo candida</i>		Albuginales	Plants	45.3	Links et al. (2011)
<i>Albugo laibachii</i>		Albuginales	Plants	35.5	Kemen et al. (2011)
<i>Lagenidium giganteum</i>		Lagenidiales	Insects	126.3	PRJNA433680
<i>Paralagenidium karlingii</i>		Lagenidiales	Mammals	49.4	PRJNA433826
<i>Bremia lactucae</i>		Peronosporales	Plants	115.9	Fletcher et al. (2019)
<i>Hyaloperonospora arabidopsidis</i>		Peronosporales	Plants	81.6	Baxter et al. (2010)
<i>Nothophytophthora valdiviana</i>		Peronosporales	Plants	84.4	Studholme et al. (2019)
<i>Peronospora belbahrii</i>		Peronosporales	Plants	35.4	Thines et al. (2019)
<i>Peronospora effusa</i>		Peronosporales	Plants	32.1	Fletcher et al. (2018)
<i>Peronospora tabacina</i>		Peronosporales	Plants	63.1	Derevnina et al. (2015)
<i>Phytophthora nicotianae</i>	1	Peronosporales	Plants	80.0	Liu et al. (2016)
<i>Phytophthora parasitica</i>	1	Peronosporales	Plants	82.4	PRJNA259235
<i>Phytophthora cactorum</i>	1a	Peronosporales	Plants	59.3	Armitage et al. (2018)
<i>Phytophthora infestans</i>	1c	Peronosporales	Plants	240.0	Haas et al. (2009)
<i>Phytophthora colocasiae</i>	2a	Peronosporales	Plants	56.6	Vetukuri et al. (2018)
<i>Phytophthora capsici</i>	2b	Peronosporales	Plants	95.2	Cui, Herlihy, Bombarely, McDowell, and Haak (2019) , Lamour et al. (2012)

Continued

Table 2 List of the 65 oomycete genome assemblies that are available at the time of writing.—cont'd

Species	Clade ^a	Order	Host	Genome Size Mb ^b	Reference ^c
<i>Phytophthora citricola</i>	2c	Peronosporales	Plants	50.3	PRJNA555328
<i>Phytophthora multivora</i>	2c	Peronosporales	Plants	40.1	Studholme et al. (2015)
<i>Phytophthora plurivora</i>	2c	Peronosporales	Plants	40.4	Vetukuri et al. (2018)
<i>Phytophthora pluvialis</i>	3	Peronosporales	Plants	53.6	Studholme et al. (2015)
<i>Phytophthora litchii</i>	4	Peronosporales	Plants	38.2	Ye et al. (2016)
<i>Phytophthora megakarya</i>	4	Peronosporales	Plants	101.2	Ali et al. (2017)
<i>Phytophthora palmivora</i>	4	Peronosporales	Plants	107.4	Ali et al. (2017)
<i>Phytophthora agathidicida</i>	5	Peronosporales	Plants	37.3	Studholme et al. (2015)
<i>Phytophthora pinifolia</i>	6b	Peronosporales	Plants	94.6	Feau et al. (2016)
<i>Phytophthora alni</i> var. <i>alni</i>	7a	Peronosporales	Plants	236.0	Feau et al. (2016)
<i>Phytophthora cambivora</i>	7a	Peronosporales	Plants	230.6	Feau et al. (2016)
<i>Phytophthora fragariae</i>	7a	Peronosporales	Plants	73.68	Gao et al. (2015)
<i>Phytophthora rubi</i>	7a	Peronosporales	Plants	74.7	Tabima et al. (2017)
<i>Phytophthora pisi</i>	7b	Peronosporales	Plants	58.9	PRJEB6298
<i>Phytophthora sojae</i>	7b	Peronosporales	Plants	95.0	Tyler et al. (2006)
<i>Phytophthora cinnamomi</i>	7c	Peronosporales	Plants	54.0	Studholme et al. (2015)
<i>Phytophthora cryptogea</i>	8a	Peronosporales	Plants	63.8	Feau et al. (2016)

<i>Phytophthora lateralis</i>	8c	Peronosporales	Plants	52.4	Feau et al. (2016)
<i>Phytophthora ramorum</i>	8c	Peronosporales	Plants	65.0	Tyler et al. (2006)
<i>Phytophthora kernoviae</i>	10	Peronosporales	Plants	39.4	Feau et al. (2016)
<i>Phytophthora taxon totara</i>		Peronosporales	Plants	55.6	Studholme et al. (2015)
<i>Phytophthium vexans</i>		Peronosporales	Plants	33.9	Adhikari et al. (2013)
<i>Plasmopara halstedii</i>		Peronosporales	Plants	75.3	Sharma et al. (2015)
<i>Plasmopara muralis</i>		Peronosporales	Plants	59.5	Dussert et al. (2019)
<i>Plasmopara obducens</i>		Peronosporales	Plants	295.3	PRJNA287843
<i>Plasmopara viticola</i>		Peronosporales	Plants	101.3	Yin et al. (2017)
<i>Pseudoperonospora cubensis</i>		Peronosporales	Plants	64.3	PRJNA80635
<i>Pseudoperonospora humuli</i>		Peronosporales	Plants	40.5	Rahman et al. (2019)
<i>Sclerospora graminicola</i>		Peronosporales	Plants	253.7	Nayaka et al. (2017)
<i>Pilaspangium apinafurcum</i>		Pythiales	Plants	37.4	Uzuhashi, Endoh, Manabe, and Ohkuma (2017)
<i>Pythium aphanidermatum</i>	A	Pythiales	Plants	35.9	Adhikari et al. (2013)
<i>Pythium arrhenomanes</i>	B	Pythiales	Plants	44.7	Adhikari et al. (2013)
<i>Pythium guiyangense</i>		Pythiales	Insects	110.2	Shen et al. (2019)
<i>Pythium insidiosum</i>	C	Pythiales	Mammals	53.2	Rujirawat et al. (2015)

Continued

Table 2 List of the 65 oomycete genome assemblies that are available at the time of writing.—cont'd

Species	Clade ^a	Order	Host	Genome Size Mb ^b	Reference ^c
<i>Pythium irregulare</i>	F	Pythiales	Plants	42.9	Adhikari et al. (2013)
<i>Pythium iwayamai</i>	G	Pythiales	Plants	43.3	Adhikari et al. (2013)
<i>Pythium oligandrum</i>	D	Pythiales	Fungi/Oomycetes	36.8	Kushwaha, Vetukuri, and Grenville-Briggs (2017a)
<i>Pythium periplocum</i>	D	Pythiales	Fungi/Oomycetes	35.9	Kushwaha et al. (2017b)
<i>Pythium splendens</i>	I	Pythiales	Plants	53.4	PRJNA548776
<i>Pythium ultimum</i> var. <i>sporangium</i>	I	Pythiales	Plants	37.7	Adhikari et al. (2013)
<i>Pythium ultimum</i> var. <i>ultimum</i>	I	Pythiales	Plants	42.8	Lévesque et al. (2010)
<i>Achlya hypogyna</i>		Saprolegniales	Crustaceans	43.4	Misner et al. (2015)
<i>Aphanomyces astaci</i>		Saprolegniales	Crustaceans	45.3	Gaulin et al. (2018)
<i>Aphanomyces euteiches</i>		Saprolegniales	Plants	56.9	Gaulin et al. (2018)
<i>Aphanomyces invadans</i>		Saprolegniales	Fish	71.4	PRJNA188082
<i>Aphanomyces stellatus</i>		Saprolegniales	Fish	62.1	Gaulin et al. (2018)
<i>Saprolegnia didina</i>		Saprolegniales	Fish	62.9	PRJNA86859
<i>Saprolegnia parasitica</i>		Saprolegniales	Fish	42.3	Jiang et al. (2013)
<i>Thraustotheca clavata</i>		Saprolegniales	Free living	39.1	Misner et al. (2015)

^aClade designation according to [Blair et al. \(2008\)](#) for *Phytophthora* and [de Cock et al. \(2015\)](#) for *Pythium*.

^bGenome size as reported in corresponding publications, otherwise the assembly size is shown.

^cNCBI BioProject accessions are shown for genome assemblies that do not have an associated publication.

Ph. ramorum and *Ph. sojae*. Analyses of genome organization showed the existence of genomic regions with high gene density and low repeat content that are syntenically conserved in the three sequenced *Phytophthora* genomes. These blocks are separated by regions with low gene density and expansions of repeat content and mobile genetic elements. These regions are typically populated with rapidly evolving effector proteins (Haas et al., 2009). This non-random distribution of effector genes in more rapidly evolving, gene-sparse regions of genomes gave rise to the model of “two-speed genomes” (Dong, Raffaele, & Kamoun, 2015).

The genome of *Pythium ultimum* var. *ultimum* was published in 2010, the first necrotrophic oomycete and first *Pythium* genome to be sequenced (Lévesque et al., 2010). *Py. ultimum* is a cosmopolitan plant pathogen with a broad host range, infecting corn, soybean, wheat and other crops (Cheung et al., 2008). The *Py. ultimum* genome is smaller (43 Mb) (Table 2) than the *Phytophthora* species that had been sequenced at that time (Lévesque et al., 2010). Genome annotation revealed an expansion of genes involved in proteolysis but a reduction in the number of genes involved in carbohydrate metabolism as well as fewer CRN genes, and no RxLR effectors (Lévesque et al., 2010). These findings led the authors to suggest that *Pythium* spp. has differences in infection mechanisms.

The genome of the obligate biotrophic downy mildew *Hyaloperonospora arabidopsidis* was also published in 2010 (Baxter et al., 2010). Compared to the sequenced *Phytophthora* species at that time, the 78 Mb *Hy. arabidopsidis* (Table 2) genome assembly showed a reduction in the number of effector genes (such as RxLRs, Crinklers, elicitors, and NLPs) and secreted degradative enzymes. The *Hyaloperonospora* genome also exhibits losses of genes involved in metabolic pathways, such as genes required for nitrogen and sulfur assimilation (Baxter et al., 2010). Together, these findings suggest a change in infection strategy and signatures of obligate biotrophy evolution. *Hy. arabidopsidis*, like most downy mildews, does not form zoospores. Comparative analysis revealed the loss of approximately 80% of *Ph. infestans* flagellar proteins in *Hy. arabidopsidis*. Gene remnants can be detected for the missing flagellar proteins, suggesting that the loss of flagella from the downy mildews was a relatively recent event (Judelson, Shrivastava, & Manson, 2012).

Two *Albugo* (white blister rust) genomes were published in 2011—*Albugo laibachii* (Kemen et al., 2011) and *Albugo candida* (Links et al., 2011). *Albugo* species are obligate biotrophic plant pathogens that belong to the Albuginales order (Fig. 2). They have evolved obligate biotrophy

independently from the downy mildew pathogens within the Peronosporales order (Kemen et al., 2011). *Al. laibachii* is a pathogen of *Arabidopsis thaliana* and *Al. candida* is a pathogen of important *Brassica* species, including canola, oilseed mustard, and cabbage family vegetables. Compared to *Hy. arabidopsidis* and the other sequenced oomycetes, the two *Albugo* genome assemblies are much smaller in size at 35–37 Mb (Table 2), contain a lower proportion of repetitive sequences and have higher gene density (Kemen et al., 2011; Links et al., 2011). A novel class of cytoplasmic effector proteins with an N-terminal “CHXC” motif was identified in *A. laibachii* (Kemen et al., 2011). Similar to *Hy. arabidopsidis*, both *Albugo* species lack a number of important metabolic enzymes, including genes required for nitrate and sulfate assimilation (Baxter et al., 2010; Kemen et al., 2011; Links et al., 2011). Moreover, both genome assemblies showed a reduction in the number of cell wall degrading enzymes and effector proteins, and in particular, no NLPs were identified. These findings illustrate similar convergent evolutionary signatures of obligate biotrophy between the *Albugo* species and *Hy. arabidopsidis* (Baxter et al., 2010; Kemen et al., 2011).

The genome of the fish pathogen *Sa. parasitica* was published in 2013, representing the first animal pathogenic oomycete genome (Jiang et al., 2013). Analysis of the 42 Mb assembly (Table 2) revealed a large divergence in gene content compared to plant pathogenic oomycetes. There was a lack of RxLRs, CRNs, and NLPs, as well as proteins involved in the breakdown of plant cell walls, such as cutinases and pectin modifying enzymes. *Sa. parasitica* was shown to possess a large arsenal of 270 proteases, one of the largest of sequenced eukaryotes at that time, these were shown to be expressed at different infection stages (Jiang et al., 2013).

The genome of the pepper and cucurbits pathogen *Phytophthora capsici* was published in 2012 (Lamour et al., 2012). The genome assembly is 64 Mb in length and is typical in terms of genome structure and gene content compared to previously sequenced *Phytophthora* genomes. However, the genome sequence revealed high levels of single nucleotide variation in addition to extensive loss of heterozygosity (LOH). LOH could be attributed to mating-type switches and loss of pathogenicity, contributing to the rapid adaption to fungicides and high levels of diversity within *Ph. capsici* populations (Lamour et al., 2012).

An additional five *Pythium* genomes (*Py. aphanidermatum*, *Py. arrhenomanes*, *Py. irregulare*, *Py. iwayami*, and *Py. ultimum* var. *sporangiiferum*) and *Phytopythium vexans* were published in 2013 and revealed compact genome sizes ranging from 34 to 45 Mb (Table 2) (Adhikari et al., 2013).

Similar to the genome sequence of *Pythium ultimum* var. *ultimum* (Lévesque et al., 2010), these *Pythium*/*Phytophthora* genomes were reported to lack RxLR effectors and possessed fewer numbers of genes involved in carbohydrate metabolism suggesting alternative virulence mechanisms (Adhikari et al., 2013). Synteny analysis of nine oomycete genomes and the distantly related diatom *Thalassiosira pseudonana* (a stramenopile outgroup) revealed a high degree of conservation of gene order between oomycetes that also extended partially with *T. pseudonana* (Adhikari et al., 2013). The animal pathogen *Py. insidiosum*, isolated from a patient with vascular pythiosis, was later sequenced with a corresponding genome assembly of 53Mb (Table 2) (Rujirawat et al., 2015). This was followed by the genome sequencing of the mycoparasites *Py. periplocum* and *Py. oligandrum* (Kushwaha et al., 2017a, 2017b), which were assembled into 36 and 37Mb genome assemblies, respectively (Table 2). Compared to plant pathogenic *Pythium* species, the mycoparasitic *Pythium* species feature expansions of carbohydrate-active enzymes (CAZymes), including carbohydrate-binding modules, carbohydrate esterases, glycoside hydrolases, glycosyltransferases, polysaccharide lyases, and redox enzymes, that potentially play important roles during mycoparasitism (Kushwaha et al., 2017a). The genome sequence of the insect parasite *Py. guiyangense* was sequenced using Illumina and PacBio platforms and resulted in a 110Mb genome assembly (Table 2), more than double the size of previously sequenced *Pythium* species (Shen et al., 2019). The large genome size is thought to be the result of interspecies hybridization as most of the *Pythium* core genes are present in two copies, likely originating from two different parental species. Genomic and experimental evidence identified CRN effector proteins that are toxic to insect cells. *Py. guiyangense* CRNs are highly divergent as all showed sequence divergence of at least 50% when compared to CRNs from plant pathogenic *Pythium* species (Shen et al., 2019).

Reconstructing the ancestor of the last common ancestor of the Stramenopiles, using whole-genome data from six pathogenic oomycetes and four non-pathogenic Stramenochromes (diatoms and alga), revealed a large ancestral genome containing approximately 10,000 genes (Seidl, Van Den Ackerveken, Govers, & Snel, 2012). Analyses of gene family evolution showed that oomycete genome evolution is under constant flux, continuously gaining and losing genes, with gene duplication events outnumbering loss events. The branch leading to the last common ancestor of the Peronosporales and the *Phytophthora* genus, in particular, is

characterized by an increased frequency of duplication events, including expansions of many gene families associated with pathogenicity including proteins with signal peptides, carbohydrate metabolizing enzymes, RxLRs and CRNs. Additionally, large numbers of species-specific gene duplication events were detected, which further contributes to the large gene family sizes of extant oomycetes (Seidl et al., 2012).

Genome sequencing of the two saprolegnian species *Achlya hypogyna* and *Thraustotheca clavata* and comparative genomic analysis of eight other oomycete genomes allowed for the reconstruction of an ancestral secretome (Misner et al., 2015). The reconstructed ancestral oomycete secretome consisted of at least 84 gene families encoding genes putatively involved in “carbohydrate metabolism and transport,” “post-translational modification, protein turnover, chaperones,” “signal transduction mechanisms” and “amino acid transport and metabolism” (Misner et al., 2015).

Genome sequences for the three *Aphanomyces* species—*Ap. astaci*, *Ap. euteiches*, and *Ap. stellatus*—revealed genome sizes ranging from 45 Mb for *Ap. astaci* to 62 Mb for *Ap. stellatus* (Table 2). Large differences in the number of protein-coding genes were observed ranging from 16,479 for *Ap. astaci* to 25,573 for *Ap. stellatus* (Gaulin et al., 2018). Comparative genomic analysis revealed that host specialization is correlated with specialized secretomes. The plant pathogen *Ap. euteiches* encodes a large arsenal of diverse cell wall degrading enzymes. In contrast, the crayfish pathogen *Ap. astaci* encodes a large number of secreted proteases and enzymes predicted to target chitin (Gaulin et al., 2018), a major component of crustacean shells.

A highly contiguous, near chromosomal level genome assembly for the downy mildew *Bremia lactucae* was achieved by combining multiple sequencing technologies, resulting in a 91 Mb assembly (Table 2), 67.3% of which was identified as being repetitive (Fletcher et al., 2019). Resequencing and flow cytometry analysis of a large number of isolates identified a high prevalence of heterokaryosis (the state of having multiple genetically distinct nuclei within cells) which can lead to rapid changes in populations including differences in virulence levels and sporulation rates (Fletcher et al., 2019). Sequencing of *Br. lactucae* adds to the growing list of downy mildew genomes available—which includes *Peronospora belbahrii*, *Peronospora effusa*, *Peronospora tabacina*, *Plasmopara halstedii*, *Plasmopara muralis*, *Plasmopara obducens*, *Plasmopara viticola*, *Pseudoperonospora cubensis*, *Pseudoperonospora humuli* and *Sclerospora graminicola* (Table 2) (Derevnina et al., 2015; Dussert et al., 2019; Fletcher et al., 2018; Nayaka et al., 2017; Rahman et al., 2019; Sharma et al., 2015; Thines et al., 2019; Yin, An, et al., 2017).

Comparative genomic and phylogenomic analysis of downy mildews and other Peronosporales lineages revealed *Bremia* and *Plasmopara* species to be more closely related to *Phytophthora* clade 1 (which includes *Ph. cactorum*, *Ph. infestans*, *Ph. nicotianae* and *Ph. parasitica*) than to the other downy mildew lineages, suggesting convergent evolution of biotrophy (Fletcher et al., 2019; McCarthy & Fitzpatrick, 2017; Sharma et al., 2015; Yin, An, et al., 2017).

Interestingly, based on hierarchical clustering of metabolic networks, oomycete species can be grouped according to their lifestyle regardless of their phylogenetic relationships (Thines et al., 2019). This includes the clustering of the distantly related *Albugo* species with the downy mildews *Hy. arabidopsidis*, *Pe. effusa*, *Pe. tabacina*, and *Pl. halstedii*. This further suggests the convergent evolution of biotrophic lifestyles. These downy mildew species were predicted to have fewer genes, enzymes, reactions, and metabolites in metabolic networks compared to other oomycete species (Thines et al., 2019). Furthermore, *Br. lactucae*, *Hy. arabidopsidis*, *Pe. belbahrii*, *Pe. effusa*, *Pe. tabacina* were shown to have undergone an extensive reduction in the number of calcium-binding and flagella associated domains. This reduction was not observed in *Plasmopara* species, which are known to produce zoospores, suggesting these missing genes are associated with the production and development zoospores (Fletcher et al., 2019, 2018; Thines et al., 2019).

The genome sequences for a large number of *Phytophthora* forest pathogens have been sequenced in recent years including *Ph. agathidicida*, *Ph. cambivora*, *Ph. cinnamomi*, *Ph. cryptogea*, *Ph. kernoviae*, *Ph. lateralis*, *Ph. multivora*, *Ph. pinifolia*, *Ph. plurivora*, *Ph. pluvialis*, *Ph. taxon totara* and the hybrid *Ph. alni* var. *alni* (Table 2) (Feau et al., 2016; Studholme et al., 2015; Vetukuri, Kushwaha, et al., 2018; Vetukuri, Tripathy, et al., 2018). Additionally, a number of important *Phytophthora* crop pathogens have been sequenced including the cacao black pod rot pathogens *Ph. megakarya* and *Ph. palmivora* (Ali et al., 2017), the strawberry pathogens *Ph. cactorum* and *Ph. fragariae* (Armitage et al., 2018; Gao et al., 2015), the litchi pathogen *Ph. litchii* (Ye et al., 2016), the raspberry pathogen *Ph. rubi* (Tabima et al., 2017), and the taro crop pathogen *Ph. colocasiae* (Vetukuri, Kushwaha, et al., 2018, Vetukuri, Tripathy, et al., 2018). The first *Nothophytophthora* genome, a sister genus of *Phytophthora*, was sequenced in 2019 and tentatively identified as *Nothophytophthora valdiviana* (Studholme et al., 2019). Such genome sequencing projects facilitate investigations into genome evolution and cataloging of effector arsenals of *Phytophthora* species with different host ranges.



3. Oomycete phylogenomics

Initial phylogenetic analyses of oomycete species were either based on single highly conserved genes, or on a small selection of highly conserved markers such as the internal transcribed spacer (ITS) region, nuclear genes (e.g., β -tubulin and translation elongation factor 1 α) and mitochondrial genes (e.g., *cox1* and *nad1*) (Martin, Blair, & Coffey, 2014). Performing phylogenetic analyses on highly conserved markers may be unable to accurately distinguish taxa at the species level. For example, some closely related *Phytophthora* species share identical ITS, *tigA*, β -tub, or *cox1* genes (Yang & Hong, 2018). These genetic markers are phylogenetically uninformative in these scenarios. Furthermore, conflicts can occur between phylogenies depending on which markers are used. The availability of whole-genome sequences has made it possible to perform whole-genome phylogenetic or phylogenomic analyses of oomycete species. Phylogenomic analyses are based on larger number of genes using genome scale data and allow for other types of phylogenetic markers such as gene duplication events.

A multi-locus phylogeny of 82 *Phytophthora* species divided the genus into 10 well supported clades (Blair et al., 2008). A follow-up analysis combining multiple nuclear and mitochondrial loci added further support for the 10 *Phytophthora* clades (Martin et al., 2014). However, the relationships between clades varied depending on which markers were used. The *Pythium* genus was divided into 10 clades (labeled A–J) based on ITS and ribosomal DNA sequences (Lévesque & De Cock, 2004). The *Pythium* genus itself is polyphyletic, separated into two monophyletic subgroupings of clades A–E and clades F–J (McCarthy & Fitzpatrick, 2017). Based on ITS sequences *Phytopyrium vexans* (previously *Pythium vexans*) was initially categorized as belonging to *Pythium* clade K (Lévesque & De Cock, 2004) but later reclassified into its own genus *Phytopyrium* belonging to the Peronosporales order based on a multi-locus analysis of nuclear and mitochondrial genes (de Cock et al., 2015), placing this species as an intermediate between *Phytophthora* and *Pythium*.

A recent phylogenomic analysis of the oomycete class used a variety of phylogenomic methods and multiple datasets including a supermatrix analysis of 352 single-copy gene families (7744 genes) ubiquitously present in 22 Peronosporales, and a supertree analysis of 2280 ubiquitous single-copy gene families (35,622 genes) as well as 8355 gene families (209,904 genes) present in at least 4 of the 37 oomycete species investigated (McCarthy &

[Fitzpatrick, 2017](#)). All methods resolved the four crown oomycete orders. Additionally, all methods suggested that *Phytophthora* is a paraphyletic genus, that gave rise to the downy mildews. Furthermore, these results show that the downy mildews are polyphyletic and that obligate biotrophy has evolved at least twice within the Peronosporales ([McCarthy & Fitzpatrick, 2017](#)). Further support for the polyphyly of downy mildews was reported in an analysis using six nuclear and mitochondrial loci of 118 taxa within the Peronosporales, including 13 downy mildews ([Bourret et al., 2018](#)). An additional phylogenomic analysis based on the concatenation of 49 conserved genes from 13 Peronosporales species (3 *Phytophthora* and 10 downy mildew) provided further evidence for the polyphyly of this group ([Fletcher et al., 2018](#)).

Complete genome sequences also allow for the identification of orthologous proteins that can be used in molecular clock analyses to estimate divergence times among species. Molecular clock analyses are particularly useful for taxa that have patchy evidence in the fossil records, such as microbial eukaryotes that are often indistinguishable due to a lack of discriminative morphological characteristics ([Matari & Blair, 2014](#)). The earliest fossil evidence for oomycetes comes from the Devonian period ~408 million years ago (MYA) ([Krings, Taylor, & Dotzler, 2011](#)). A molecular clock analysis of 12 oomycetes and 6 outgroups was performed using 40 orthologs involved in gene expression regulation, that are highly conserved across 18 genomes ([Matari & Blair, 2014](#)). Three molecular clock methods were employed (strict clock, UCLD relaxed clock and random local clock) and calibrated with fossil evidence from oomycetes and diatoms. The results suggest that the oomycetes arose some 430–400 MYA, with the two major branches leading to the Peronosporaleans and Saprolegnialeans diverging 225–190 MYA ([Matari & Blair, 2014](#)). These findings indicate that the oomycetes arose later than their hosts and that the evolution of pathogenicity may have been influenced by environmental changes or facilitated by events such as HGT from pathogenic bacteria and fungi ([Matari & Blair, 2014](#)). A follow-up analysis was performed using the random local clock model with the same calibration points and same dataset except for the addition of three *Aphanomyces* genomes (*Ap. astaci*, *Ap. euteiches* and *Ap. stellatus*) ([Gaulin et al., 2018](#)). This analysis estimated that *Aphanomyces* diverged from other Saprolegniales species more than 100 MYA, and the three *Aphanomyces* species diverged from each other more than 50 MYA indicating relatively recent host specialization of animal and plant pathogenic *Aphanomyces* species ([Gaulin et al., 2018](#)).

Here we present an updated phylogeny of the oomycete class based on the currently available genome sequences (Table 2) using a phylogenomic approach. We include the genome of the non-oomycete Stramenopile *Hyphochytrium catenoides* as an outgroup (Leonard et al., 2018). As the majority of genome sequences deposited in NCBI GenBank do not have associated gene models, we used Benchmarking Universal Single-Copy Orthologs (BUSCOs) as phylogenetic markers (Waterhouse et al., 2018). BUSCOs are highly conserved genes that are expected to be found in a genome only as a single copy. BUSCO analysis using the “Alveolata-Stramenopiles” dataset revealed 102 BUSCO families that are present and single-copy in 84% of the 66 genome assemblies, i.e., they are present and single-copy in at least 56 of the 66 species. Each BUSCO family was individually aligned using MUSCLE (Edgar, 2004). Alignments were subsequently trimmed using trimAl with the parameter “-automated1” which uses a heuristic method to decide which trimming method is most appropriate (Capella-Gutierrez, Silla-Martinez, & Gabaldon, 2009). Trimmed alignments were then concatenated, resulting in a supermatrix of 44,739 amino acid residues. Maximum-likelihood analysis was performed using IQ-TREE (Nguyen, Schmidt, Von Haeseler, & Minh, 2015) under the JTT + F + R7 model, which was the best fit model according to ModelFinder (Kalyaanamoorthy, Minh, Wong, von Haeseler, & Jermini, 2017). Support for each node was calculated based on 100 bootstrap replicates. The phylogeny was visualized and annotated using the Interactive Tree of Life (iTOL) (Letunic & Bork, 2007).

Our phylogeny recovered all genera with generally high bootstrap support (Fig. 2) and is in broad agreement with previous phylogenetic and phylogenomic studies. All *Phytophthora* species were recovered in their expected clades (Fig. 2). The relationships within the Peronosporales order, including between individual *Phytophthora* clades, are in complete agreement with a smaller phylogenomic analysis of Peronosporales species based on 18 BUSCO proteins (Fletcher et al., 2019). Our phylogeny groups *Phytophthora* clades 6 (*Ph. pinifolia*) and 7 as sister clades, which is in agreement with a previous phylogeny based on seven nuclear loci and also a multispecies coalescent approach based on two nuclear and four mitochondrial loci (Martin et al., 2014), although we obtained a low bootstrap support value of 49% (Fig. 2). The relationships between *Phytophthora* clades 2–5 in our phylogeny differ from previous nuclear and mitochondrial phylogenies (Blair et al., 2008; Martin et al., 2014). Our phylogeny groups *Phytophthora* clades 2 and 3 (*Ph. pluvialis*) together to the exclusion of clade

4 (Fig. 2). Although we obtained low bootstrap support (52%) for the grouping of clades 2 and 3, it agrees with previous phylogenomic analyses (Fletcher et al., 2019; McCarthy & Fitzpatrick, 2017). Our results confirm that *Phytophthora* is a paraphyletic genus, suggesting that clades 1–4 are more closely related to each other than to those in clades 5–10 (Fig. 2). *Phytophthora* clades 3, 5, and 6 currently only have one sequenced representative species each. *Phytophthora* clade 9 is currently the only *Phytophthora* clade lacking genomic data. Sequencing of multiple species from each *Phytophthora* clade will likely lead to increased resolution as to the relationships between clades.

Based on the current genome sequences available, it appears that the downy mildews are a polyphyletic group that arose from *Phytophthora* species, with two phylogenetically distinct clades that convergently evolved obligate biotrophy (Fig. 2). This is in agreement with previous studies (Bourret et al., 2018; Fletcher et al., 2019, 2018; McCarthy & Fitzpatrick, 2017). The first clade consists of *Bremia* and *Plasmopara* which are closely related to *Phytophthora* clade 1 (100% bootstrap support) (Fig. 2). The second clade contains *Hyaloperonospora*, *Sclerospora*, *Pseudoperonospora*, and *Peronospora* species, which groups with *Ph. taxon totara* (100% bootstrap support) (Fig. 2). Therefore, obligate biotrophy has evolved at least twice within the Peronosporales order. Obligate biotrophy has evolved independently a third time in the Albuginales order (Fig. 2).

Nothophytophthora was placed as a sister to the *Phytophthora* genus (Fig. 2). *Pp. vexans* is placed intermediate to the Peronosporales and Pythiales orders (Fig. 2). As seen in previous studies, the *Pythium* genus is polyphyletic with clades A–D grouping together, and clades F–I grouping together (Fig. 2). Genomic data is currently not available for *Pythium* clades E, H or J. The insect pathogen *Py. guiyangense* is grouped with the plant pathogenic *Py. irregulare* and *Py. iwayamai* (100% bootstrap support), while the mammal pathogen *Py. insidiosum* is grouped with the plant pathogenic *Py. aphanidermatum* and *Py. arrhenomanes* (77% bootstrap support) (Fig. 2). This suggests that animal pathogenicity has evolved independently multiple times within the *Pythium* genus.

La. giganteum is grouped with *Pythium* clades A–D and not *Paralagenidium karlingii* (Fig. 2). This agrees with a six-gene phylogeny that groups *La. giganteum* with *Pythium* species to the exclusion of *Pa. karlingii*, indicating that *Paralagenidium* is phylogenetically unrelated to the main clades of the oomycetes (Spies et al., 2016). It also agrees with phylogenies based on ITS and cox2 sequences (Vilela, Humber, Taylor, & Mendoza, 2019).

However, our phylogeny suggests that *Pa. karlingii* is even more distantly related as it places it intermediate to the Albuginales and Saprolegniales orders with 100% bootstrap support (Fig. 2), this is in agreement with the phylogeny shown in Beakes and Thines (2016). The previous two phylogenetic analyses (Spies et al., 2016; Vilela et al., 2019) did not include Albuginales sequences. The availability of more genome sequences and whole gene sets will help to further clarify the relationships among contentious oomycete clades.



4. Oomycete mitochondrial genomes

As discussed above, mitochondrial genes have been useful for understanding the evolutionary relationships between oomycete species. Several oomycete mitochondrial genomes have been sequenced in full and analyzed, revealing variation in mitochondrial structure and gene content across oomycete lineages. Sequencing of the *Saprolegnia ferax* mitochondrion revealed a densely packed ~47 kb circular genome (Fig. 3A) that encodes 37 protein and rRNA coding genes (18 respiratory chain proteins, 16 ribosomal proteins, the import protein secY, and the large and small ribosomal subunits) and 25 tRNA genes (Grayburn, Hudspeth, Gane, & Hudspeth, 2004). An 8618 kb inverted repeat was identified separating the genome into two single-copy regions (Fig. 3A). The mitochondrion of *Ph. infestans* was determined to be a ~38 kb genome (Fig. 3B) that is A + T rich (76%) and has high gene density with more than 95% of the genome coding (Paquin et al., 1997). The mitochondrial genome sequences of *Ph. ramorum* (Fig. 3C) and *Ph. sojae* were determined to be ~39 kb and ~43 kb, respectively (Martin, Bensasson, Tyler, & Boore, 2007). Similar to *Sa. ferax*, both *Phytophthora* mitochondrial genomes encode 37 protein and rRNA coding genes and 26 (*Ph. ramorum*) or 25 (*Ph. sojae*) tRNA genes that specify 19 amino acids. *Ph. ramorum* possess a 1150 bp inverted repeat encoding an additional tRNA that is not present in *Ph. sojae*. Otherwise, the gene order between the two mitochondrial genomes is conserved. Comparison with the *Ph. infestans* mitochondrial genome revealed high conservation of genome collinearity except for two inversions that include 3 and 19 coding regions. Conservation of gene order also extended partially to that of *Sa. ferax*.

The mitochondrial genomes of several clade 1c *Phytophthora* species were sequenced to understand the relationships within the clade, including *Ph. infestans*, *Ph. phaseoli*, *Ph. ipomoeae*, *Ph. mirabilis* and two lineages of *Ph. andina* (Lassiter et al., 2015). Mitochondrial genomes within clade 1c are

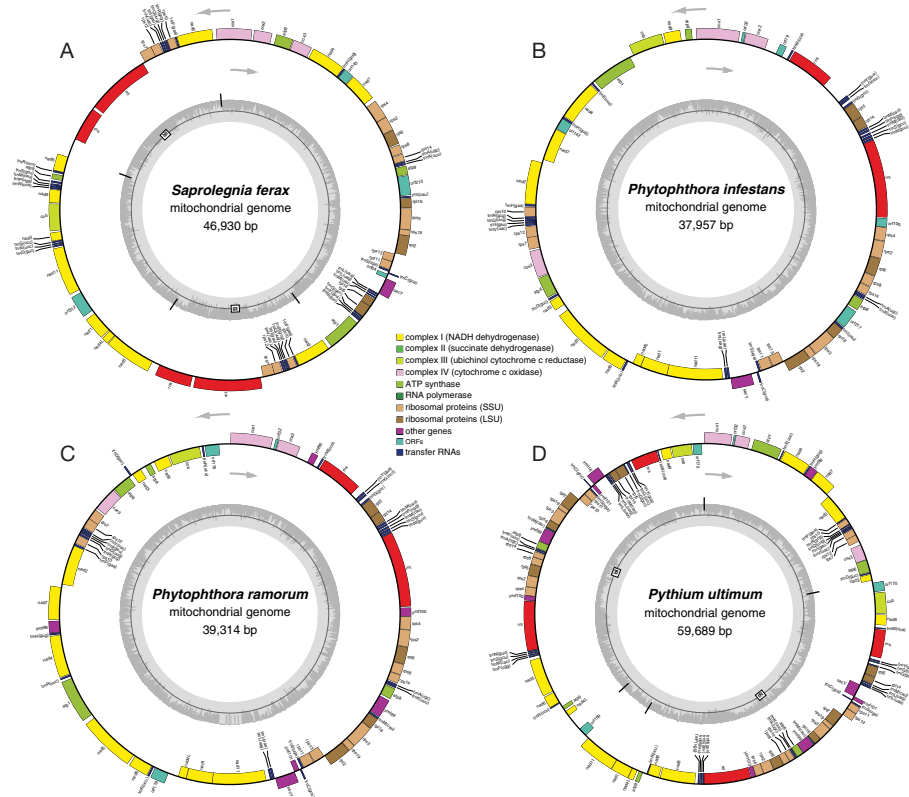


Fig. 3 Structures of representative oomycete mitochondrial genomes. (A) *Saprolegnia ferax* (NC_005984.1), (B) *Phytophthora infestans* (NC_002387.1), (C) *Phytophthora ramorum* (NC_009384.1), and (D) *Pythium ultimum* (NC_014280.1). Mitochondrial genomes are not drawn to scale. Transcriptional orientation is indicated by arrows. GC content is shown in the inner circles. Inverted repeats are indicated with "IR". The small inverted repeat (1,150 bp) in *Ph. ramorum* is not shown.

highly conserved in terms of size, all mitochondrial assemblies are approximately 38 kb and only varied by 179 bp. Gene order is identical among all species and sequence identity of proteins is greater than 99% (Lassiter et al., 2015). The mitochondrial genome of *Py. ultimum* was shown to be larger at ~60 kb (Fig. 3D). The increase in size is due to a large inverted repeat of ~22 kb (Fig. 3D). The genome encodes the same set of protein and RNA encoding genes but many are duplicated in the inverted repeat region (Lévesque et al., 2010). The mitochondrial genome of *Py. insidiosum* was found to be similarly large at ~55 kb, containing two large inverted repeats (Tangphatsornruang et al., 2016).

Genome sequencing of the *Ph. nicotianae* mitochondrion revealed a ~37.5 kb sequence that is identical to the previously sequenced *Phytophthora* mitochondrial genomes in terms of gene content (Yuan, Feng, Zhang, & Zhang, 2017). Comparative genomic analysis of the *Ph. nicotianae* mitochondrion and 13 other oomycete mitochondrial genomes showed that large inverted repeats are absent in the mitochondria of *Phytophthora* species. This analysis showed that a ~10 kb inversion, containing 8 tRNAs and 11 genes, is common to *Ph. andina*, *Ph. impomoeae*, *Ph. infestans*, *Ph. mirabilis* and *Ph. phaseoli* relative to *Ph. nicotiana*, *Ph. polonica*, *Ph. ramorum* and *Ph. sojae*. Furthermore, while overall gene content is similar between oomycetes, the overall mitochondrial genome size and gene copy number are higher in the Pythiales and Saprolegniales due to the presence of duplications in inverted repeat regions (Yuan et al., 2017). The mitochondrial genome of *Pe. effusa* was determined to be ~41 kb in length and shares the same organization with the *Pe. tabacina* mitochondrial genome, except for a small inverted repeat less than 900 bp that is present in *Pe. effusa* (Derevnina et al., 2015; Fletcher et al., 2018). Sequencing of *Ps. humuli* revealed a 39 kb mitochondrial genome that is AT-rich (77.8%) and gene dense with coding regions representing 90% of the genome. The gene order of the *Ps. humuli* mitochondria is identical to *Ps. cubensis* but the small ribosomal subunit is encoded in the opposite direction compared to *Pe. tabacina* and *Phytophthora* species (Rahman et al., 2019).



5. The impact of horizontal gene transfer on oomycete evolution

Horizontal gene transfer (HGT), or lateral gene transfer (LGT), is the nonvertical transfer of genetic material between different species (Savory, Leonard, & Richards, 2015). HGT can have significant evolutionary consequences, such as facilitating recipient species to adapt to different

ecosystems or exploit new hosts. Before oomycete genomes were first sequenced, it was known that HGT played an important role in the evolution of oomycetes. Phylogenetic analysis of *Ph. infestans* EST sequences identified an endopolygalacturonase gene (*pipg1*), encoding an enzyme involved in pectin breakdown, that's most closely related homologs belonged to fungi suggesting a possible HGT event from fungi to *Phytophthora* (Torto, Rauser, & Kamoun, 2002). Sequencing of the *Ph. ramorum* and *Ph. sojae* genome (Tyler et al., 2006) facilitated more in-depth analyses of HGT which led to the identification of four HGT events from ascomycete fungi to *Phytophthora* with strong phylogenetic evidence (Richards et al., 2006). Interestingly, each of the four genes are likely to be involved in osmotrophy-related functions, implying that HGT may have played a role in the convergent evolution of osmotrophy and filamentous growth between fungi and oomycetes. There is also evidence of HGT events from bacteria to oomycetes, including secreted cutinases (important virulence factors involved in the breakdown of the plant cuticle) that appear to have been transferred from Actinobacteria to oomycetes and later duplicated, with 16 copies being found in the *Ph. sojae* genome (Belbahri, Calmin, Mauch, & Andersson, 2008). Another analysis that examined metabolic enzymes from eukaryotic genomes showed that 2% of metabolic enzymes in the genomes of *Ph. ramorum* and *Ph. sojae* potentially originated via HGT (Whitaker, McConkey, & Westhead, 2009).

The availability of more oomycete genomes has allowed for more comprehensive, whole-genome scans to identify genes that may have been gained via HGT. Similarly, the availability of more non-oomycete genomes has led to increased taxon sampling in databases adding further support for the validity of HGT events. Phylogenetic analysis of four oomycetes genomes (*Hy. arabidopsidis*, *Ph. infestans*, *Ph. ramorum* and *Ph. sojae*) using a database of 795 (173 eukaryotic and 622 prokaryotic) genomes identified 34 gene transfers between fungi and oomycetes (Richards et al., 2011). Interestingly, 62%–76% of genes identified as originating via HGT from fungi in the four analyzed species possess a predicted secretion signal, representing between 2.7% and 7.6% of the total predicted secretomes of these species. Many of the identified genes have functions associated with the breakdown of plant cell walls and the uptake of nitrogen, nucleic acids, phosphate and sugars from the environment (Richards et al., 2011). This adds further support to the hypothesis that HGT events from fungi have played a part in the convergent evolution of osmotrophy and filamentous growth between fungi and oomycetes. Genome analysis of *Sa. parasitica*

led to the identification of five gene families (four of which are secreted) that appear to have been gained by *Sa. parasitica* via HGT from bacteria or animals (Jiang et al., 2013). An additional six HGT events were reported from the genome sequences of *Ac. hypogyna* and *Th. clavata*, all of which are predicted to be secreted and involved in pathogenicity or carbohydrate metabolism (Misner et al., 2015).

Reanalysis of 48 HGT gene families based on the 23 oomycetes genomes that were available in 2015 highlighted several important findings (Savory et al., 2015). For example, 33 (69%) of the 48 HGT families are predicted to be secreted and 40 (83%) of the 48 HGT families appear to have a fungal origin. Only seven cases of HGT could be mapped back to the ancestor of the four crown oomycete orders, suggesting that HGT played a limited role in early oomycete evolution. HGT appears to have had a greater impact on plant pathogenic oomycetes, with 33 HGT events identified within the *Phytophthora*, *Hy. arabidopsidis* and *Pythium* clade, compared to only five in the branch leading to the Saprolegniales order (Savory et al., 2015). Interestingly, many of the HGT derived genes have not only become fixed in the recipient genomes but have been duplicated, sometimes multiple times. For example, *Pythium* and *Phytopyrium* species have a mean of 2.1 copies of each HGT derived gene, whereas *Phytophthora* species have a mean of 4.4 (Savory et al., 2015). Acquisition of genes via HGT can potentially change the phenotype of the recipient and also provide genetic material that has the potential to evolve novel or expanded functions. Detailed functional analyses of transporter proteins that were transferred to oomycetes before the divergence of Peronosporales and Saprolegniales revealed an HGT derived paralogue belonging to *Py. aphanidermatum* that has evolved an expanded substrate range enabling it to uptake not only dicarboxylic acid (the ancestral function) but also tricarboxylic acid (Savory, Milner, Miles, & Richards, 2018).

Analysis of EST sequences from *Py. oligandrum* identified a homolog of a type 2 NLP from bacteria (Horner, Grenville-Briggs, & van West, 2012). Type 2 NLPs were previously thought to be absent in oomycetes and only found in fungi and bacteria. A follow-up analysis of effector proteins in 37 oomycete genomes using network and phylogenetic methods identified type 2 NLPs in three oomycete species—*Py. oligandrum*, *Pilaspangium apinafurcum* and *Pp. vexans* (McGowan & Fitzpatrick, 2017). Phylogenetic analysis suggested that the genes were likely gained via HGT from a Proteobacterial source and later duplicated with 2 copies in *Pp. vexans*, 6 copies in *Pi. apinafurcum* and 17 copies present in *Py. oligandrum*.

An additional five instances of HGT from bacteria to oomycetes were reported in another study focusing on 14 plant pathogenic oomycete genomes including a putative secreted protein, a class II fumarase, an oxidoreductase, an alcohol dehydrogenase, and a hydrolase (McCarthy & Fitzpatrick, 2016).

Based on the genome analyses conducted to date, it is clear that HGT has played a significant role in oomycete genome evolution. In particular, HGT has had a major impact on the secretomes of plant pathogenic oomycetes such as *Phytophthora*. Furthermore, convergent evolution between fungi and oomycetes was likely driven, in part, by HGT. As more genome sequences become available it will be possible to more accurately place the timing of putative HGT events, e.g., in an oomycete ancestor or specific to particular oomycete lineages, and also to rule out possible effects of poor taxon sampling.



6. Genome mining for oomycete effectors

Oomycete species are notorious for secreting large arsenals of effector proteins that perform a wide array of functions during infection. Genome sequencing of oomycete species has facilitated genome mining to identify effector proteins which has led to many studies comparing effector repertoires between species and evolutionary analyses of effector families. The first step in identifying effector proteins is usually predicting which proteins are secreted using tools such as SignalP (Almagro Armenteros et al., 2019) to identify putative signal peptides. Transmembrane domains are then annotated using TMHMM (Krogh, Larsson, von Heijne, & Sonnhammer, 2001). Proteins that contain predicted transmembrane helices downstream of the signal peptide are usually discarded. It is important to note, that unconventionally secreted proteins (i.e., secreted proteins that lack a signal peptide and are signaled for secretion by some other mechanism) will be overlooked using this approach. Additionally, false positives may be reported. Therefore, the gold standard method for identifying secreted proteins is coupling bioinformatics methods with experimental techniques such as mass spectrometry (Meijer et al., 2014) or the yeast secretion trap system (Lee et al., 2006). ApoplastP is a machine learning classifier that can be used to predict if effector proteins localize to the plant apoplast (Sperschneider, Dodds, Singh, & Taylor, 2018). Many effector families contain conserved domains that can be annotated using hidden Markov model (HMM) searches against databases such as InterPro (Finn et al., 2017) or Pfam (Finn et al., 2016), for example, elicins (PF00964) and NLPs (PF05630).

Other effector families may have conserved positionally constrained motifs that can be identified using string searches or regular expression searches. For example, the RxLR family contains an N-terminus “RxLR” motif (where “x” means any amino acid) downstream of the signal peptide cleavage site. Similarly the CRN family contains a conserved N-terminus “LxLFLAK” motif which is usually followed downstream by an “HVLVxxP” motif (Haas et al., 2009). More robust searches can be carried out to identify effectors with divergent motifs by building HMMs based on the results from regular expression searches. Novel effector proteins have also been identified due to being located in gene-sparse, repeat-rich regions of the genome with close proximity to transposable elements (Raffaele, Win, Cano, & Kamoun, 2010). Additionally, many effector proteins are found in clusters of tandemly duplicated genes (McGowan, Byrne, & Fitzpatrick, 2019). Effector-like proteins can also be identified by performing sequence similarity searches against databases of known effectors, for example, using BLAST (Altschul et al., 1997) to identify homologs of experimentally verified effectors in the Pathogen-Host Interaction database (PHI-base) (Urban et al., 2017). The physio-chemical properties of a protein can also be used to identify effectors, for example, many effectors are small (low molecular weight), and cysteine-rich (Sperschneider et al., 2015; Sperschneider, Dodds, Singh, & Taylor, 2018). The cysteine residues might be involved in disulfide bridges, increasing the stability and lifespan of effector proteins in the plant apoplast which contains a large number of degradative proteases (Kamoun, 2006). Genome-wide cataloging of effector proteins has revealed differences in effector repertoires between species with different hosts, some of which are discussed below.

6.1 Apoplastic effectors

Apoplastic effectors are secreted by the pathogen and exert their pathogenic activity outside of the host cell (Wawra et al., 2012). Oomycete genomes encode large arsenals of secreted degradative enzymes that breakdown host cell components facilitating hyphal penetration of host cells. These degradative enzymes include CAZymes which modify and breakdown carbohydrates. In addition to allowing entry into host cells, the breakdown of host carbohydrates also makes nutrients available for the pathogen to grow. Phytopathogenic oomycetes encode large arsenals of secreted CAZymes to facilitate the breakdown of plant cell wall components, including cellulases to metabolize cellulose, cutinases to degrade cutin, pectinases to degrade

pectin, endoglucanases and β -glucosidases to degrade xyloglucan, and α -glucosidases, α -amylases, α -glucoamylases, and starch-binding modules to metabolize starch (Zerillo et al., 2013). As cellulose is also one of the main components of oomycete cell walls, it is thought that most oomycete cellulases are involved in oomycete cell wall metabolism and only few are involved in the breakdown of plant cell walls. However, they are still important for infection as a *Ph. infestans* cellulose synthase was shown to be involved in the formation of appressoria and required for infection (Grenville-Briggs et al., 2008). Furthermore, proteins with cellulose-binding domains are enriched in the secretome of many *Phytophthora* species suggesting a role in infection (McGowan & Fitzpatrick, 2017). Chitinases and chitin-binding proteins are also expanded in some oomycete genomes including *Ap. astaci*, *Py. oligandrum*, *Sa. didina* and *Sa. parasitica* (Jiang et al., 2013; McGowan & Fitzpatrick, 2017). As oomycete cell walls contain very little to no chitin, this suggests that oomycete chitin modifying enzymes are involved in the breakdown of exogenous chitin. This is particularly significant for the expansion of chitinases in species such as *Py. oligandrum* and *Ap. astaci*, which parasitize fungi and crayfish, respectively. Other types of degradative enzymes include proteases which are also thought to be involved with host cell degradation (Haas et al., 2009). For example, proteases are highly expanded in the animal pathogens *Sa. parasitica* and *Py. guiyangense* and may facilitate cuticle penetration (Jiang et al., 2013; Shen et al., 2019). Interestingly, oomycetes also secrete protease inhibitors to counteract defense proteases produced by the host in response to infection (Tian et al., 2006), highlighting the co-evolutionary arms race between pathogens and their hosts.

Many secreted oomycete proteins or oomycete cell wall/membrane constituents are recognized by the host and trigger a host defense response upon recognition (Oome et al., 2014). Such molecules are referred to as microbe-associated molecular patterns (MAMPs). Well-characterized oomycete MAMPs include elicitors, transglutaminases, and cellulose-binding elicitor lectins (CBELs). Elicitors are known to bind lipids and sequester sterols from host plants, allowing some pathogenic oomycetes to overcome their inability to synthesize their own sterols (Kamoun, 2006). Transglutaminases facilitates the cross-linking of protein-bound glutamine and lysine residues, strengthening structures such as cell walls and conferring resistance to proteolysis (Raaymakers & Van den Ackerveken, 2016). CBEL proteins are known to activate expressions of host defense genes and elicit necrosis and are important for cell wall structure (Raaymakers & Van den Ackerveken, 2016).

Other well studied apoplastic effectors include NLPs and the PcFs. NLPs have a broad taxonomic distribution across the tree of life with homologs found in bacteria, fungi, and oomycetes (Seidl & Van den Ackerveken, 2019). NLPs are known to induce ethylene accumulation leading to rapid tissue necrosis and are associated with the switch to necrotrophy in *Phytophthora* species. Some NLPs have been reported to be noncytotoxic but instead, act as MAMPs (Oome et al., 2014). NLPs are highly expanded in some oomycete species, in particular, some *Phytophthora* species have up to 80 copies (McGowan & Fitzpatrick, 2017). NLPs are completely absent in some species such as *Albugo*, *Aphanomyces* and *Saprolegnia* (Kemen et al., 2011; Links et al., 2011; McGowan & Fitzpatrick, 2017). In contrast to NLPs, PcF proteins are present in lower copy numbers, with 16 identified in *Ph. infestans*, 8 in *Ph. sojae* and only 1 in *Ph. ramorum* (Haas et al., 2009).

Pcf proteins are small, cysteine-rich proteins that are known to induce plant cell necrosis (Orsomando et al., 2001). Pcf proteins appear to be unique to Peronosporales species based on the currently available genome sequences.

6.2 Cytoplasmic effectors

Oomycete cytoplasmic effectors differ from apoplastic effectors in that they are secreted and translocated into host cells. Three main classes of oomycete cytoplasmic effectors have been identified—RxLRs, CRNs and CHXC effectors. RxLR effectors are so named because they contain a highly conserved “RxLR” motif in their N-terminal domain. This is often followed downstream by an “EER” motif in many RxLRs (Whisson et al., 2007). RxLR C-terminal domains are typically highly divergent although many contain conserved structural folds caused by the presence of one or more “WY” domains (Win et al., 2012). RxLRs are highly expanded in the Peronosporales order but were not detected at all in *Aphanomyces*, *Pythium* or *Saprolegniales* species (Adhikari et al., 2013; Gaulin et al., 2018; Jiang et al., 2013; Lévesque et al., 2010). However, small numbers of RxLR and RxLR-like effectors have been detected in the two *Albugo* genomes (Kemen et al., 2011; Links et al., 2011), making their origin unclear. RxLR effectors are particularly abundant in the genomes of *Phytophthora* species, for example, *Ph. infestans* is predicted to encode 563 RxLRs (Haas et al., 2009), while *Ph. palmivora* and *Ph. megakarya* are predicted to encode 991 and 1181 RxLRs, respectively (Ali et al., 2017). Many *Phytophthora* RxLRs are expressed in early infection stages and play

a role in modulating and suppressing the host immune response (Yin et al., 2017). However, the function and molecular mechanisms for most RxLRs are unknown. While the function of most RxLRs is unknown, the subcellular location of a large number of *Ph. infestans* RxLRs was recently determined. *Ph. infestans* RxLRs were shown to localize to diverse subcellular locations when they enter plant cells, with most localizing to the host cytoplasm, nucleus or plasma membrane (Wang et al., 2019). Furthermore, most of the RxLRs under consideration were shown to enhance colonization. The mechanism of translocation into host cells is unclear but some RxLRs have been shown to enter host cells independent of additional pathogen-encoded machinery (Dou et al., 2008). Recent work has shown that the haustorium is involved in the delivery of apoplastic and cytoplasmic effectors both by conventional and nonconventional secretory pathways (Wang et al., 2017, 2018).

Currently the origin of oomycete RxLR effectors is unclear. Interestingly, comparative genomic and syntenic analysis using the Oomycete Gene Order Browser (OGOB) (McGowan et al., 2019) reveals a conserved *Ph. infestans* RxLR effector (SFI4 or PITG_09585) that appears to have been present in the ancestor of the four crown oomycete orders. SFI4 localizes to the host nucleus-cytoplasm and reduces flg22-induced pFRK1-Luc activation in tomato protoplasts, enhancing *Ph. infestans* colonization (Zheng et al., 2014). SFI4 is also highly expressed during infection of potato (Yin, Gu, et al., 2017). In OGOB, SFI4 is in a pillar with orthologs from 17 other species (Fig. 4A). An ortholog was not identified in *Al. candida* or *Al. laibachii*, suggesting that it may have been lost by these species. As orthologs are found in Peronosporales, Pythiales and Saprolegniales orders, it suggests that this is an ancient RxLR gene locus that was present in an ancestral oomycete species. All protein sequences in this pillar show a high degree of sequence similarity (Fig. 4B) and are reciprocal best hits to each other in a BLASTp search. Furthermore, all orthologs in this pillar show evidence of microsyntenic conservation (Fig. 4C), adding further evidence that they are legitimate orthologs. SignalP analysis predicts that 17 out of the 18 proteins in this pillar contain a signal peptide. Multiple sequence alignment reveals the presence of a conserved RxLR motif in all orthologs in this pillar (Fig. 4B). All orthologs contain a KDEL or KDEL-like motif at the C-terminus, a motif usually involved in endoplasmic reticulum (ER) retention (i.e., non-secretion), however, it is possible that it is masked. A homolog of PITG_09585 was previously detected in *Py. oligandrum* (Horner et al., 2012) but was not considered a bona fide RxLR effector

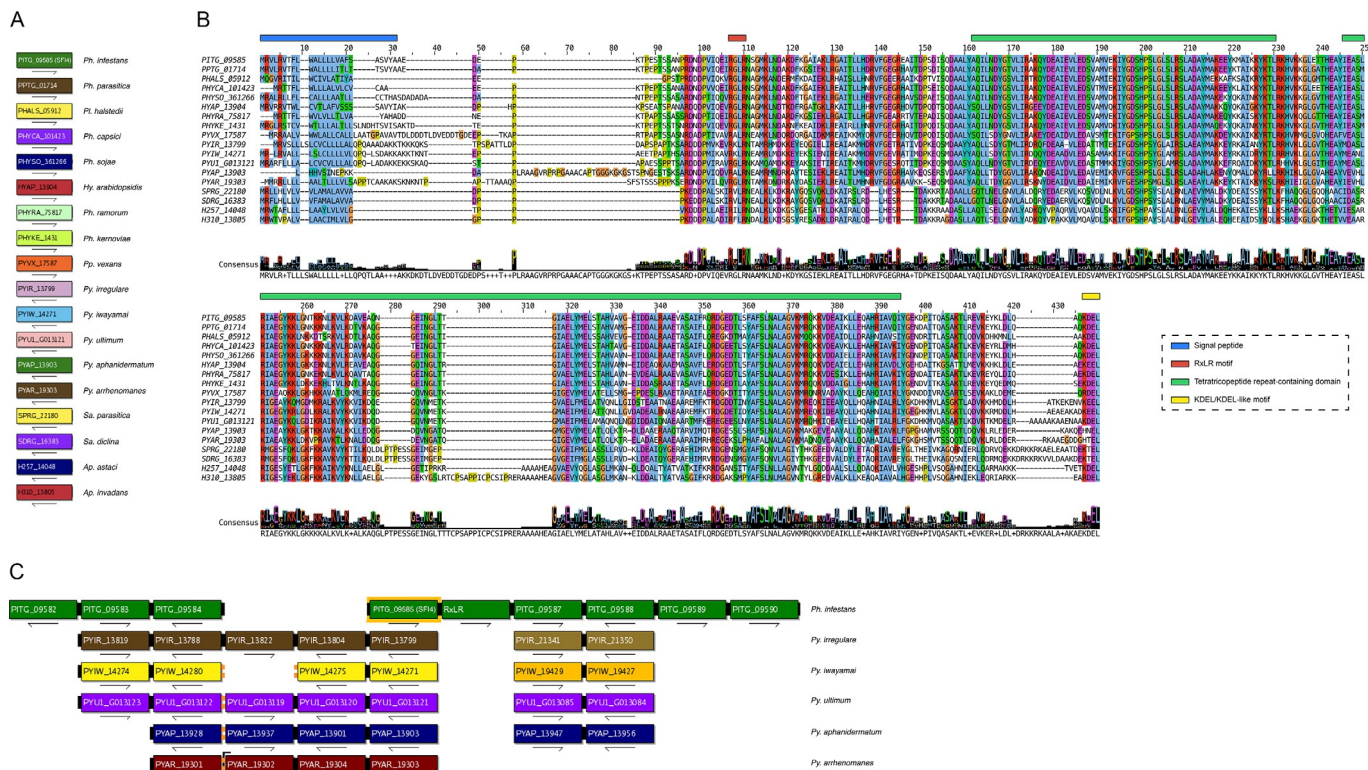


Fig. 4 An ancient conserved oomycete RxLR locus. (A) *Ph. infestans* SFI4 (PITG_09585) has orthologs in other *Phytophthora*, *Hyaloperonospora*, *Phytophthora*, *Pythium*, *Saprolegnia* and *Aphanomyces* species. (B) Multiple sequence alignment of PITG_09585 and its orthologs show extensive sequence similarity and the presence of a “RxLR” motif. (C) Genomic context of SFI4 and its orthologs visualized in OGOB showing that it is microsyntenically conserved. A solid connector between two genes indicates that the two genes are adjacent in the genome, two small bars indicate that they are within five genes of each other. Connectors that are colored orange denote an inversion. A bracket around a gene box indicates the end of a contig/scaffold. PITG_09585 is highlighted with a gold border. For illustrative purposes, only PITG_09585 and its *Pythium* orthologs are shown. Full microsynteny of other orthologs can be examined on OGOB.

due to the presence of the KDEL C-terminal motif. In addition to *Ph. infestans* SFI4, a number of the orthologs have evidence of transcription during infection. The ortholog in *Hy. arabidopsidis* (HYAP_13904 or RxLR5) was identified during expressed sequence tag (EST) sequencing of infected *Arabidopsis* tissue (Cabral et al., 2011). The *Ph. capsici* ortholog (PHYCA_101423) has evidence of expression during infection of *Nicotiana benthamiana* in RNA-Seq experiments (Chen, Xing, Li, Tong, & Xu, 2013) and during infection of tomato in microarray experiments (Jupe et al., 2013). Additionally, the *Pl. halstedii* ortholog (PHALS_05912) was identified in an RNA-Seq analysis of infected sunflower (Sharma et al., 2015). Interestingly, comparative RNA-seq analysis of *Ph. infestans* and *Py. ultimum* has shown that the two orthologs (PITG_09585 and PYU1_G013121) have similar expression patterns during potato tuber colonization (Ah-Fong, Shrivastava, & Judelson, 2017). Whether the conserved orthologs in *Pythium*, *Aphanomyces* and *Saprolegnia* function as effectors warrants further investigation to understand their importance. Together, these data suggest that the RxLR class of effectors is more ancient than previously thought and may have evolved in an ancestral oomycete species prior to their proliferation in Peronosporales species.

CRNs are named after their crinkling and necrosis-inducing activity. CRN proteins have highly conserved N-terminal domains containing a signal peptide and a “LxLFLAK” motif that mediates translocation into host cells (Schornack et al., 2010). The end of the N-terminus is marked by a highly conserved “HVLVxxP” motif. CRNs are modular proteins that have highly diverse C-terminal domains (Haas et al., 2009). In contrast to RxLRs, CRNs are thought to be a more ancient class of effectors as they have been detected across a wide range of oomycetes including *Albugo*, *Aphanomyces*, downy mildews, *Phytophthora* and *Pythium* (Gaulin et al., 2018; Kemen et al., 2011; Links et al., 2011; Schornack et al., 2010). CRNs were not detected in the genome of *Sa. parasitica* (Jiang et al., 2013). CRNs are also highly expanded in the genomes of some *Phytophthora* species, with 196 CRNs annotated in *Ph. infestans* and 100 in *Ph. sojae* (Haas et al., 2009). CRNs include some of the most highly expressed effector genes before and during infection (Haas et al., 2009). Several CRNs have been reported to target the host nucleus (Schornack et al., 2010). Interestingly, highly divergent CRNs were identified in the genome of the insect pathogen *Py. guiyangense* and some were shown to be toxic in insect cells (Shen et al., 2019). Similar to RxLRs, CRNs have undergone rapid evolution, expansion, and diversification. For example, the genomes of *Ph. megakarya* and *Ph. palmivora* were

where shown to encode 152 and 137 CRNs, respectively, but only 30 of these are core-orthologs shared between these two closely related pathogens (Ali et al., 2017). Many annotated CRNs lack conventional N-terminal signal peptides. For example, only 58% of annotated *Ph. cactorum* CRNs possess a canonical signal peptide and only 60 out of the predicted 139 (43%) CRN proteins in *Ph. plurivora* have a signal peptide (Armitage et al., 2018; Vetukuri, Tripathy, et al., 2018). A large number of CRN and RxLR pseudogenes were annotated in the genome of *Ph. infestans* suggesting the prevalence of rapid gene birth and death, possibly driven by the co-evolutionary arms race between pathogen and host, and an effort to evade host recognition (Haas et al., 2009).

Sequencing of the *Al. laibachii* genome led to the identification of a novel class of CHXC effectors (Kemen et al., 2011). Similar to the other characterized cytoplasmic effectors, the *Albugo* CHXC effectors contain a conserved “CHxC” motif within 50 amino acids of the signal peptide cleavage site that was shown to facilitate effector translocation into host cells (Kemen et al., 2011). A total of 29 CHXC effector candidates were annotated in the *Al. laibachii* genome. The “CHxC” motif was also significantly enriched in the secretome of *Al. candida* where a total of 40 CHXC effector candidates were identified, none of which had homologs in *Phytophthora* or *Hyaloperonospora* (Links et al., 2011).



7. Oomycete OMICS studies

Genome sequencing of oomycete species has also facilitated other high throughput “OMICS” analyses such as proteomics and transcriptomics. Such analyses have revealed insights into oomycete infection mechanisms, secretome content, cell structure, metabolism, and nutritional strategies. Additionally, proteomic and transcriptomic data have been invaluable for improving the quality of oomycete genomes via the annotation and validation of predicted genes.

7.1 Oomycete proteomics studies

The majority of proteomics studies to date have focused on *Phytophthora* species. Comparative proteomic analysis between mycelium and germinating cysts of *Ph. ramorum* and *Ph. sojae* was carried out to identify proteins involved in vegetative and infection stages (Savidor et al., 2008). In total, 3897 proteins were identified from *Ph. ramorum* and 2970 from *Ph. sojae*. An average of 14% of identified proteins contained a signal peptide, 42 of

which from *Ph. sojae* and 46 from *Ph. ramorum* contained an RxLR motif within the first 30–60 residues suggesting they belong to the RxLR effector family. 686 proteins were identified as being differentially expressed between germinating cysts and mycelium in *Ph. ramorum*. This number was 513 for *Ph. sojae* (Savidor et al., 2008). Proteins upregulated in germinating cysts were involved in functions related to cytoskeleton, protein synthesis and the transport and metabolism of lipids (including many proteins involved in the β -oxidation pathway). Proteins upregulated in mycelium were involved in functions related to the transport and metabolism of amino acids, carbohydrates, and other small molecules. These findings revealed insights into infection, growth and nutritional strategies of *Phytophthora* species. They suggested that germinating cysts catabolize lipids (via the β -oxidation pathway), generating the energy required for protein synthesis for germ tube formation used in infection initiation. Upon entry into the host, *Phytophthora* switches to vegetative mycelial growth, generating energy via glycolysis to synthesize amino acids and other molecules required for survival inside host tissues (Savidor et al., 2008). Comparative proteomic analysis of *Ph. pisi* and *Ph. sojae* revealed proteomic differences that may contribute to host specificity between these two closely related pathogens (Hosseini et al., 2015). A total of 2775 proteins from *Ph. pisi* and 2891 proteins from *Ph. sojae* were identified. Similar findings were reported with regards to nutritional strategy differences between hyphae and germinating cysts (Hosseini et al., 2015; Savidor et al., 2008). Proteomic profiling of *Ph. capsici* identified 599 proteins with significantly altered expression in response to the fungicide SYP-14288 (Cai et al., 2019). The majority of affected proteins had functions related to carbohydrate metabolism, energy metabolism, metabolism of other amino acids, amino acid metabolism, transport, and catabolism.

The *Ph. infestans* genome encodes 372 genes predicted to be protein kinases, comprising 2% of the total gene set, suggesting that phosphorylation plays an important role in the lifecycle of *Ph. infestans* (Resjö et al., 2014). A large-scale phosphoproteomics analysis of six life stages of *Ph. infestans* (hyphae, sporangia, zoospores, cysts, germinated cysts, and appressoria) was performed to identify phosphorylated peptides (Resjö et al., 2014). A total of 2922 phosphopeptides were identified. Among the phosphorylated peptides were 35 CRN-derived phosphopeptides. Many CRNs were phosphorylated at multiple sites, across several life stages indicating a potential role beyond inducing necrosis (Resjö et al., 2014). Quantitative proteomic analysis of the same six life stages identified over 10,000 peptides

corresponding to 2061 proteins (Resjö et al., 2017). In particular, 59 proteins were significantly more abundant in appressoria and germinating cysts, i.e., pre-infection stages of the life cycle. The majority of these proteins are involved in transport, energy and amino acid metabolism, redox maintenance and signaling (Resjö et al., 2017). Interestingly, this set of proteins with increased abundance in pre-infection stages also included many proteins involved in cell wall synthesis, maintenance, and adhesion. Transient silencing of three of these putative cell wall proteins resulted in abnormal phenotypes and an impaired ability to infect potato leaves, suggesting an important role in the infection process (Resjö et al., 2017). *Ph. infestans* cell-wall associated proteins from three life stages (germinating cysts with appressoria, sporulating mycelium, and non-sporulating mycelium) were also identified using a mass spectrometry approach, resulting in the identification of 31 proteins (Grenville-Briggs et al., 2010). All of the cell-wall associated proteins of germinating cysts with appressoria and some from mycelia were classified as effectors or MAMPs which could potentially trigger a host immune response.

Mass spectrometric analyses of *Ph. infestans* grown in seven different types of growth media was performed to characterize and validate proteins belonging to the secretome and extracellular proteome of *Ph. infestans* (Meijer et al., 2014). In total, 283 proteins were identified in the extracellular media confirming they are bona fide extracellular proteins, of which 227 contained a signal peptide. Among the identified proteins were 20 RxLRs, 13 CRNs, 11 elicitors, and 5 necrosis-inducing proteins (Meijer et al., 2014). Thirty one proteins were found to contain a signal peptide and a single transmembrane domain (most of which were located in the C-terminus), suggesting that they are membrane proteins that are proteolytically shed via sheddases, explaining their presence in the extracellular medium (Meijer et al., 2014). The proteomics approach facilitated the reannotation and correction of many gene models, the N-terminus of many were extended revealing signal peptides that weren't previously annotated. A similar approach was carried out to characterize the secretome of *Ph. plurivora* when stimulated with root exudate from *Fagus sylvatica* resulting in the identification of 272 proteins, 60% of which contained signal peptides (Severino et al., 2014). The secretome was enriched with functions related to enzymatic activity such as hydrolases, oxidoreductases, and transferases. Twenty one proteins were found to be differentially abundant following treatment with root exudate (Severino et al., 2014).

While the majority of oomycete proteomic analyses have focused on *Phytophthora* species, several analyses have been performed for other taxa. For example, comparative proteomic analysis of *Py. insidiosum* revealed 212 proteins and 124 proteins that were found in higher or lower abundance, respectively, when grown at 37°C compared to 25°C (Rujirawat et al., 2018). The majority of highly upregulated proteins were predicted to be involved in transport and metabolism of amino acids, carbohydrates, lipids and nucleotides, post-translational modification, protein turnover, and chaperones. These proteins may facilitate the high-temperature tolerance of *Py. insidiosum* during infection of mammals (Rujirawat et al., 2018). Quantitative proteomic analysis of four life stages (mycelium, primary cysts, secondary cysts, and germinated cysts) of *Sa. parasitica* grown in vitro identified a total of 2423 unique proteins across the four life stages (Srivastava, Rezinciuc, & Bulone, 2018). Compared to the three cyst stages, 133 proteins were found in increased abundance in the mycelium with functions related to amino acid and carbohydrate metabolism enriched. Conversely, 110 proteins were found in increased abundance in the three cyst stages compared to the mycelium with an enrichment of functions related to signal transduction, translation, ribosomal structure and biogenesis (Srivastava et al., 2018).

7.2 Oomycete transcriptomics studies

Transcriptomic analyses (i.e., RNA-seq) are now routinely performed alongside genome sequencing as the sequenced transcripts can be incorporated during gene calling steps and to validate existing gene models. Many transcriptomics studies have been carried out for oomycete species to identify transcriptional remodeling during infection or after exposure to chemical treatment. Comparative transcriptomics analyses between different species have also been performed to identify differences or similarities between species.

RNA-seq analysis of various life stages in two *Ph. infestans* isolates led to the mapping and validation of approximately 16,000 genes (90%) (Ah-Fong, Kim, & Judelson, 2017). Large-scale transcriptome remodeling was detected at each life stage with the biggest differences observed during the transition from hyphae to sporangia where more than 4200 genes were upregulated, more than 1350 of which were detected at greater than 100-fold increased abundance. Genes encoding calcium-binding proteins, flagellar proteins, ion channels, and signaling proteins were upregulated in sporangia. Most

metabolic pathways were downregulated after sporulation but later reactivated upon the germination of cysts (Ah-Fong, Kim, & Judelson, 2017). Similarly, RNA-seq analysis of *Ph. capsici* identified a large number of stage-specific genes including effector families and metabolic pathways, revealing proteins that are important during pre-infection (Chen et al., 2013). Transcriptome analysis of *Ph. litchei* mycelia, sporangia, and zoospores identified 19,267 unigenes, of which 490 were predicted to be pathogenicity-related proteins, including 128 RxLRs, 35 elicitors, 29 NLPs and 22 CRNs (Sun et al., 2017). The *Ph. litchei* unigenes were clustered into 9685 orthologous groups, 105 gene families did not have orthologs in the other four oomycete species under consideration in the study, suggesting that they may be novel genes.

Comparative transcriptomic analysis was performed to identify transcriptional differences between *Ph. infestans* and *Py. ultimum* during infection of potato tubers (Ah-Fong, Shrivastava, & Judelson, 2017). This is an interesting pair of species for comparison, as they both infect potato and have different lifestyles. *Ph. infestans* is a hemibiotroph that begins infection with a biotrophic phase whereby it requires a living host for colonization. Later in the infection process, *Ph. infestans* switches to a highly destructive necrotrophic phase. In comparison, *Py. ultimum* is a necrotroph that immediately induces host cell death upon infection. *Ph. infestans* was found to have a higher number of stage-specific genes. In particular, a much larger proportion of *Ph. infestans* genes were shown to have ≥ 4 -fold expression change between early and late infection (45% in *Ph. infestans* compared to only 9% in *Py. ultimum*), this could be attributed to the switch from biotrophy to necrotrophy that *Ph. infestans* undergoes during late infection. The evolution of necrotrophy and hemibiotrophy could be ascribed to species-specific genes, expansion and contraction of orthologous gene families, and differences between the timing and level of expression of orthologs (Ah-Fong, Shrivastava, & Judelson, 2017). RNA-seq analysis of the saprotroph *Salisaplia sapeloensis* was performed in comparison to eight other plant pathogenic oomycetes with different lifestyles (biotrophic, hemibiotrophic and necrotrophic) (de Vries, de Vries, Archibald, & Slamovits, 2019). Results show that the saprotrophic and pathogenic oomycetes possess similar repertoires for colonization but exhibit different expression patterns. Furthermore, *Salisaplia sapeloensis* was shown to possess a smaller effector arsenal. These findings indicate that the evolution of oomycete lifestyles is influenced not only by gene content but also shifts in gene regulatory networks (de Vries et al., 2019).

Transcriptomic methods have also proven useful in understanding how oomycetes respond to chemical treatments and biocontrol agents. RNA-seq of *Ph. infestans* in response to the phenazine-1-carboxylic acid (PCA) producing *Pseudomonas fluorescens* showed that more than 200 genes were significantly differentially expressed with more than a threefold change following PCA treatment (Roquigny, Novinscak, Arseneault, Joly, & Filion, 2018). Differentially expressed genes were predicted to be involved in many processes, including oxidoreduction activity, phosphorylation mechanisms and transmembrane transport activity. Transcriptional changes were also identified in effector genes even in the absence of a host plant. These findings suggest that PCA exposure results in growth repression which leads to transcriptomic changes in *Ph. infestans* (Roquigny et al., 2018). RNA-seq analysis of *Ph. parasitica* in response to the fungicide dimethomorph identified significant differential expression of 832 genes, of which 365 were up-regulated and 467 down-regulated, including many genes associated with the cell membrane and wall synthesis (Hao et al., 2019). RNA-seq of *Sa. parasitica* following treatment with copper sulfate showed that 310 genes were upregulated and 556 genes were down-regulated (Hu et al., 2016). Functional annotation of differentially expressed genes indicates that copper sulfate inhibits the growth of *Sa. parasitica* by affecting multiple biological processes including energy biogenesis, metabolism and protein synthesis (Hu et al., 2016).

Tissue-specific and host induced genes from *Sa. parasitica* were identified via RNA-seq of multiple life stages as well as infected fish cell lines (Jiang et al., 2013). In particular, the results suggested that kinases play an important role during the infection process, as of the large kinome (543 kinases) of *Sa. parasitica*, 10% were upregulated greater than fourfold in germinating cysts compared to mycelia. Similarly, the large arsenal of proteases (270) was shown to be expressed in waves at different stages during infection, indicating an important role in the infection process (Jiang et al., 2013). RNA-seq of *Ap. euteiches* infecting *Medicago truncatula* showed that adaption to plant hosts is correlated with the expression of specialized secretomes (Gaulin et al., 2018). Genes involved in carbohydrate metabolism and proteolysis were upregulated during infection. Furthermore, three times as many secreted protein-encoding genes were upregulated during infection, the majority of which encode proteases, glycoside hydrolases and polysaccharide lyases (Gaulin et al., 2018).

Dual transcriptomic analyses can be employed to characterize the infection process of a pathogen and the response of the host to that pathogen.

Dual transcriptomic time-course analysis of *Ph. palmivora* infecting *Nicotiana benthamiana* identified 2441 differentially expressed *Ph. palmivora* genes and 6950 differentially expressed *Ni. benthamiana* genes in response to the pathogen (Evangelisti et al., 2017). The pathogen was shown to undergo sharper transcriptional remodeling in comparison to the host plant which was characterized by steady up or downregulation. A large number of putative *Ph. palmivora* effectors were identified including 143 cell wall degrading enzymes, 140 RxLRs, 59 proteases, 42 elicitors, 28 small cysteine-rich proteins, 24 NLPs and 15 CRNs (Evangelisti et al., 2017). Genes linked to abiotic stress, biosynthesis, defense, hormone metabolism, protein modification, and transcriptional regulation were upregulated in *Ni. benthamiana*. Genes associated with cell division, cellulose biosynthesis and photosynthesis were downregulated during infection. These results suggest that *Ni. benthamiana* responds to *Ph. palmivora* infection by transcriptional remodeling and post-translational reprogramming which activates defense and stress responses (Evangelisti et al., 2017).



8. Tools for oomycete genomics

Compared to other taxonomic groups, there are few dedicated tools available to study oomycete genomes. However, there have been several recent developments, including EumicrobeDB (<http://www.eumicrobedb.org>; last accessed December 1, 2019), a database that hosts 26 oomycete genome sequences and a large number of bioinformatics tools (Panda et al., 2018). FungiDB (<https://fungidb.org>; last accessed December 1, 2019) also hosts genomic data for 21 oomycete species (Basenko et al., 2018). The Oomycete Gene Order Browser (OGOB) (<https://ogob.ie>; last accessed December 1, 2019) was recently published and hosts genomic data for 20 oomycete species, including syntenically curated orthology inferences and bioinformatics tools that facilitate comparative genomic analyses and a browser for examining syntenic conservation of protein-coding genes between multiple species (McGowan et al., 2019). Additional databases dedicated to oomycetes include *Phytophthora*-ID (<http://phytophthora-id.org>; last accessed December 1, 2019) (Grünwald et al., 2011) and OomyceteDB (<http://oomycetedb.cgrb.oregonstate.edu>; last accessed December 1, 2019), which are curated databases that host genetic marker sequences for identifying oomycete species. There are also few dedicated tools to functionally annotate oomycete genes. For example, EffectorP is a tool that can be used to predict

effector proteins from fungal secretomes using a machine learning classifier (Sperschneider, Dodds, Gardiner, Singh, & Taylor, 2018). With the growing number of experimentally verified oomycete effectors, similar approaches could be used to build machine learning classifiers for oomycete effectors.

Identifying BUSCOs is one of the most commonly used methods for assessing genome assembly completeness (Waterhouse et al., 2018). Currently, the most specialized BUSCO dataset available for oomycete genomes is the “Alveolata-Stramenopiles” dataset. An issue with this is that it only contains 234 BUSCO proteins based on a highly diverse set of 24 species, only seven of which are oomycetes. Other species in this dataset include the Alveolates—*Plasmodium falciparum* and *Toxoplasma gondii*. Including distantly related lineages when identifying orthologs reduces the number of universally present single-copy orthologs. This may result in an inaccurate assessment of genome assembly completeness. A dedicated dataset for the oomycetes, or better, for individual oomycete lineages/genera, would provide a more accurate representation of genome and gene space completeness. For example, analysis of the 20 oomycete genomes hosted on OGOB (McGowan et al., 2019) using OrthoFinder (Emms & Kelly, 2019) identifies 643 ubiquitously conserved single-copy orthologs. Furthermore, taxonomically restricting this dataset to the genomes of eight more closely related Peronosporales species (*Hy. arabidopsidis*, *Ph. capsici*, *Ph. infestans*, *Ph. kernoviae*, *Ph. parasitica*, *Ph. ramorum*, *Ph. sojae*, and *Pl. halstedii*) identifies 2231 ubiquitously conserved single-copy orthologs. Additional highly conserved markers can also be considered when assessing genome completeness. For example, the Fungal Genome Mapping Pipeline (FGMP) was recently developed to assess genome completeness of fungal genome assemblies, taking into account not only ubiquitous single-copy gene families but also ubiquitous multi-copy gene families and highly conserved non-coding regions (Cissé & Stajich, 2019). Using the OrthoFinder analysis above, there are 53 gene families that are ubiquitously multi-copy (i.e., all genomes contain more than one copy) across the 20 oomycete genomes hosted on OGOB, and 83 across the eight Peronosporales genomes. Including ubiquitously duplicated genes in genome assembly assessment can potentially identify genome misassemblies such as collapsed duplications or repetitive regions. With the availability of large numbers of oomycete genome sequences available, similar sophisticated methods could be developed to assess genome assembly quality and completeness of oomycete genomes.



9. Oomycetes in the post-genomic era

The quality of the 65 genomes reviewed herein varies greatly. Oomycete genomes can be difficult to assemble due to their relatively large size, high proportions of repeat content and high levels of heterozygosity in certain species. Genome completeness of the 65 genome assemblies, assessed using BUSCO v3 (Waterhouse et al., 2018) with the Stramenopiles/Alveolata BUSCO dataset, ranges from 99.10% to 42.80% (mean = 89.32%; median = 94.00%) (Fig. 5), showing that most oomycete genomes are highly complete in terms of expected gene content. The percentage of single-copy BUSCOs present ranges from 98.70% to 16.70% (mean = 80.83%; median = 90.6%) (Fig. 5), indicating that several genomes have a large number of BUSCOs that are present in multiple copies. While this may represent legitimate multiple copies and duplication events, such is the case in the hybrid *Py. guiyangense* which contains duplicates for 81.6% of BUSCOs (Fig. 5), it also likely represents haplotypes that weren't fully collapsed or misassemblies of repetitive sequences that cannot be assembled fully. Most oomycete genomes have very low fragmented BUSCO scores, ranging from 0% to 4.5% (mean = 1.3%; median = 0.9%) (Fig. 5), suggesting that gene fragmentation isn't a problem. Many of the currently available oomycete genome assemblies are highly fragmented, with sequences split across thousands or even tens of thousands of short contigs or scaffolds. The majority of oomycete genomes have been sequenced using short-read Illumina sequencing only. Illumina sequencing produces high yields of high-quality reads. However, the reads are short with a length range between 50 and 250 nucleotides. Short reads cannot span the length of repetitive regions of the genome as the repetitive regions are typically longer than the reads, resulting in highly fragmented genome assemblies with many short contigs. Long-read sequencing technologies such as PacBio and Oxford Nanopore Technologies (ONT) have the potential to generate higher-quality assemblies in terms of contiguity and completeness of repetitive regions. PacBio sequencing produces sequencing reads with average read lengths of over 10,000 bp and maximum read lengths of over 60,000 bp (Rhoads & Au, 2015). ONT can sequence full-length fragments of DNA, detecting bases as they pass through a nanopore. Long-reads from PacBio and ONT platforms are more likely to span repetitive regions leading to more contiguous oomycete genome assemblies that have longer and fewer contigs. Long-read sequencing also facilitates more comprehensive comparative genomic and

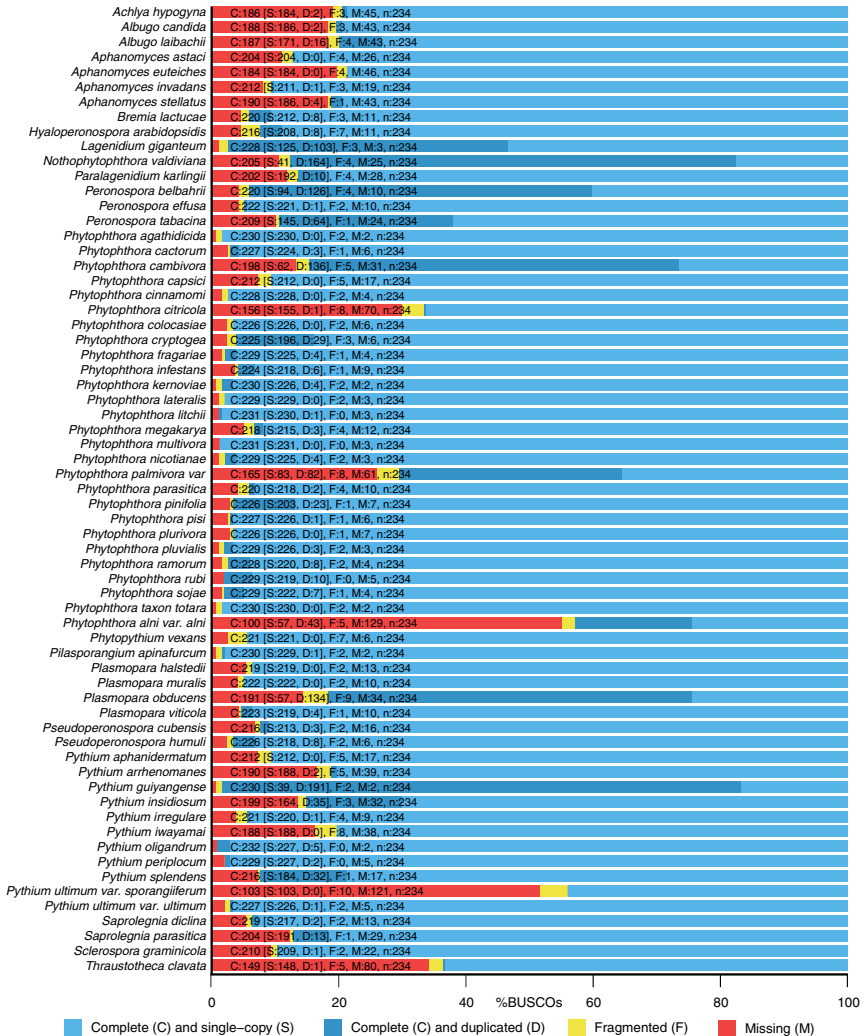


Fig. 5 Distribution of BUSCO completeness scores across the 65 Oomycete genomes, assessed using the 234 BUSCOs from the “Alveolata-Stramenopiles” dataset.

syntenic analyses as larger structural variants, such as large inversions or translocations, can be detected. Long-read sequencing presents a trade-off as generated reads have a higher error rate compared to Illumina reads, and library construction and sequencing are more expensive with a higher cost per base. Hybrid sequencing approaches can be undertaken in which long-reads or long-read assemblies are corrected and polished with high coverage,

high-quality short-reads. This approach combines the benefits of long-read and short-read sequencing, producing high-quality, more complete and more contiguous assemblies.

Several oomycete genome sequencing projects have already taken advantage of long-read sequencing technologies. Sequencing of a highly virulent *Ph. ramorum* isolate (ND886) using PacBio long-read sequencing generated a haplotype-phased assembly that is much more contiguous than the reference (Pr102) assembly (302 contigs versus 2576 contigs) (Malar et al., 2019). Additionally, the PacBio assembly contains a much higher proportion of repeat content than the reference assembly (48% versus 29%) showing the ability of long-read sequences to span and assemble repetitive sequences. The average read length was 10,570 bp and the longest read was 50,801 bp. The reference *Ph. ramorum* genome (Pr102) was also re-sequenced using the PacBio platform to a total of 80X coverage with an average read length of 14,000 bp, in combination with Illumina short-reads (Malar, Yuzon, Panda, Kasuga, & Tripathy, 2019). The updated assembly is 5 Mb larger than the previous reference assembly (Tyler et al., 2006), is more contiguous (1512 scaffolds versus 2576 scaffolds), contains a higher proportion of repetitive content (54.4% versus 29.08%) and an additional 3360 genes were reported (Malar, Yuzon, Panda, et al., 2019). Resequencing of *Ph. capsici* using an ONT MinION long-reads resulted in a more contiguous assembly (424 scaffolds) that was 95 Mb in length (~30 Mb larger than the reference assembly) (Cui et al., 2019). The increased assembly size corresponds to an increase in repeat content that was captured using long-read sequencing. A single MinION flow-cell produced ~10 Gb of data corresponding to 70X coverage. The N50 of the unassembled reads was 11,507 bp, the average read length was 7114 bp and the longest read was 99,577 bp. Interestingly the authors noted that the improved assembly was generated in only 9 days (Cui et al., 2019). Therefore the ONT MinION sequencing platform brings us closer to real-time field sequencing during pathogen outbreaks, allowing for rapid identification and tracking of pathogens as infection occurs.

Recent long-read sequencing efforts have also revealed novel insights into oomycete biology and genetics. Resequencing of *Ph. sojae* using ONT and PacBio long-read sequencing coupled with chromatin immunoprecipitation sequencing (ChIP-Seq) led to the identification of centromeres (Fang et al., 2020). The identified *Phytophthora* centromeres were large, transposon rich and without nucleotide bias, showing divergence from other organisms in the SAR supergroup that have relatively short

and simple centromeric sequences. Copia-like transposon (CoLT) elements that are highly enriched in the *Ph. sojae* centromeres were identified and shown to be conserved in *Ph. citricola* and *Br. lactucae*, presenting a novel feature that may be used to predict centromeres in other oomycete species (Fang et al., 2020). Telomeres were identified at single ends of 13 contigs in the long-read assembly. It is not yet accurately known how many chromosomes are present in *Ph. sojae*, due to difficulties in resolving karyotypes using pulse-field gel electrophoresis caused by large genome size and potentially similar chromosome sizes. Based on the identification of centromeres and telomeres in the updated *Ph. sojae* assembly, it is estimated that *Ph. sojae* has 12–14 chromosomes (Fang et al., 2020).

Resequencing multiple diverse strains of the same species followed by de novo genome assembly will allow for future pan-genomic analyses of oomycete species. The pan-genome is the union of “core” conserved genes and all “accessory” non-conserved genes across all strains of a species. Large numbers of isolates have already been re-sequenced for a number of oomycete species. For example, resequencing of 107 *Ph. ramorum* isolates revealed rapid evolution within lineages (Dale et al., 2019). Novel genotypic diversity within lineages was caused by mitotic recombination leading to loss of heterozygosity affecting 2698 genes. Accelerated evolution was detected in non-core regions which are enriched in effector genes and transposons. Furthermore, positive selection was observed in 8.0% of RxLRs and 18.8% of CRNs. It is estimated that of the four lineages (EU1, EU2, NA1, and NA2), EU1 and NA1 diverged 0.75 MYA, NA2 diverged from EU1 and NA1 1.06 MYA, and EU2 diverged from the other lineages some 1.3 MYA (Dale et al., 2019). Future resequencing studies of diverse strains of individual oomycete species will facilitate pan-genomic analyses which can provide insights into strain-level variation of gene content, genetic differences in pathogenicity aggressiveness, mechanisms of fungicide resistance and differences in host ranges. This will enable oomycete research to transition from the genomics era to the pan-genomics era.



10. Conclusions and future outlook

In line with recent advances in next-generation sequencing technologies and drastic decreases in the cost of whole-genome sequencing, there has been an increased pace of oomycete genome sequencing. Oomycete genomics has revealed fundamental insights into the biology and evolution of oomycetes. Based on the available genomic data, it is clear that HGT has

played a significant role in shaping oomycete genome evolution, in particular, it has had a major impact in the evolution of plant pathogenicity and the convergent evolution of similar traits between oomycetes and fungi. Phylogenomic studies have helped to better understand the evolutionary relationships between oomycete species. Genome-wide cataloging of oomycete effectors has led to the identification of large, diverse apoplastic and cytoplasmic effector families which facilitates experimentation to better understand the disease process and identify future antimicrobial targets.

With the increasing number of oomycete genomes there is a need for more dedicated tools to be developed to study oomycete genomics. While many genome assemblies are available for the crown oomycete orders, there is a dearth of genomic data available for more basal oomycete species. Furthermore, there is a lack of genomic data for non-pathogenic oomycetes or saprotrophic oomycetes that play key ecological roles in natural environments. Future sequencing of basal oomycetes will reveal further insights into oomycete genome evolution and the origin of oomycetes and the evolution of pathogenicity.

Acknowledgments

J.M. is funded by a postgraduate scholarship from the Irish Research Council, Government of Ireland (grant number GOIPG/2016/1112). We acknowledge the DJEI/DES/SFI/HEA Irish Centre for High-End Computing (ICHEC) for the provision of computational facilities and support.

References

- Adhikari, B. N., Hamilton, J. P., Zerillo, M. M., Tisserat, N., Lévesque, C. A., & Buell, C. R. (2013). Comparative genomics reveals insight into virulence strategies of plant pathogenic oomycetes. *PLoS One*, 8(10), e75072. <https://doi.org/10.1371/journal.pone.0075072>.
- Ah-Fong, A. M. V., Kim, K. S., & Judelson, H. S. (2017). RNA-seq of life stages of the oomycete *Phytophthora infestans* reveals dynamic changes in metabolic, signal transduction, and pathogenesis genes and a major role for calcium signaling in development. *BMC Genomics*, 18(1), 198. <https://doi.org/10.1186/s12864-017-3585-x>.
- Ah-Fong, A. M. V., Shrivastava, J., & Judelson, H. S. (2017). Lifestyle, gene gain and loss, and transcriptional remodeling cause divergence in the transcriptomes of *Phytophthora infestans* and *Pythium ultimum* during potato tuber colonization. *BMC Genomics*, 18(1), 764. <https://doi.org/10.1186/s12864-017-4151-2>.
- Ali, S. S., Shao, J., Lary, D. J., Kronmiller, B. A., Shen, D., Strem, M. D., et al. (2017). *Phytophthora megakarya* and *Phytophthora palmivora*, closely related causal agents of cacao black pod rot, underwent increases in genome sizes and gene numbers by different mechanisms. *Genome Biology and Evolution*, 9(3), 536–557. <https://doi.org/10.1093/gbe/evx021>.
- Almagro Armenteros, J. J., Tsirigos, K. D., Sønderby, C. K., Petersen, T. N., Winther, O., Brunak, S., et al. (2019). SignalP 5.0 improves signal peptide predictions using deep neural networks. *Nature Biotechnology*, 37(4), 420–423. <https://doi.org/10.1038/s41587-019-0036-z>.

- Altschul, S. F., Madden, T. L., Schäffer, A. A., Zhang, J., Zhang, Z., Miller, W., et al. (1997). Gapped BLAST and PSI-BLAST: A new generation of protein database search programs. *Nucleic Acids Research*, 25(17), 3389–3402. <https://doi.org/10.1093/nar/25.17.3389>.
- Armitage, A. D., Lysøe, E., Nellist, C. F., Lewis, L. A., Cano, L. M., Harrison, R. J., et al. (2018). Bioinformatic characterisation of the effector repertoire of the strawberry pathogen *Phytophthora cactorum*. *PLoS One*, 13(10), 1–24. <https://doi.org/10.1371/journal.pone.0202305>.
- Basenko, E., Pulman, J., Shanmugasundram, A., Harb, O., Crouch, K., Starns, D., et al. (2018). FungiDB: An integrated bioinformatic resource for fungi and oomycetes. *Journal of Fungi*, 4(1), 39. <https://doi.org/10.3390/jof4010039>.
- Baxter, L., Tripathy, S., Ishaque, N., Boot, N., Cabral, A., Kemen, E., et al. (2010). Signatures of adaptation to obligate biotrophy in the *Hyaloperonospora arabidopsidis* genome. *Science*, 330(6010), 1549–1551. <https://doi.org/10.1126/science.1195203>.
- Beakes, G. W., Glockling, S. L., & Sekimoto, S. (2012). The evolutionary phylogeny of the oomycete “fungi”. *Protoplasma*, 249(1), 3–19. <https://doi.org/10.1007/s00709-011-0269-2>.
- Beakes, G. W., & Thines, M. (2016). *Hyphochytriomycota and oomycota*. In J. M. Archibald, A. G. B. Simpson, C. H. Slamovits, L. Margulis, M. Melkonian, D. J. Chapman, & J. O. Corliss (Eds.), *Handbook of the protists* (pp. 1–71). Cham: Springer International Publishing. https://doi.org/10.1007/978-3-319-32669-6_26-1.
- Belbahri, L., Calmin, G., Mauch, F., & Andersson, J. O. (2008). Evolution of the cutinase gene family: Evidence for lateral gene transfer of a candidate *Phytophthora* virulence factor. *Gene*, 408(1–2), 1–8. <https://doi.org/10.1016/j.gene.2007.10.019>.
- Benhamou, N., le Floch, G., Vallance, J., Gerbore, J., Grizard, D., & Rey, P. (2012). *Pythium oligandrum*: An example of opportunistic success. *Microbiology*, 158(11), 2679–2694. <https://doi.org/10.1099/mic.0.061457-0>.
- Benson, D. A., Cavanaugh, M., Clark, K., Karsch-Mizrachi, I., Lipman, D. J., Ostell, J., et al. (2012). GenBank. *Nucleic Acids Research*, 41(D1), D36–D42. <https://doi.org/10.1093/nar/gks1195>.
- Blair, J. E., Coffey, M. D., Park, S. Y., Geiser, D. M., & Kang, S. (2008). A multi-locus phylogeny for *Phytophthora* utilizing markers derived from complete genome sequences. *Fungal Genetics and Biology*, 45(3), 266–277. <https://doi.org/10.1016/j.fgb.2007.10.010>.
- Bourret, T. B., Choudhury, R. A., Mehl, H. K., Blomquist, C. L., McRoberts, N., & Rizzo, D. M. (2018). Multiple origins of downy mildews and mito-nuclear discordance within the paraphyletic genus *Phytophthora*. *PLoS One*, 13(3) e0192502. <https://doi.org/10.1371/journal.pone.0192502>.
- Burki, F., Roger, A. J., Brown, M. W., & Simpson, A. G. B. (2019). The new tree of eukaryotes. *Trends in Ecology & Evolution*, 35, 1–13. <https://doi.org/10.1016/j.tree.2019.08.008>.
- Cabral, A., Stassen, J. H. M., Seidl, M. F., Bautor, J., Parker, J. E., & Van den Ackerveken, G. (2011). Identification of *Hyaloperonospora arabidopsidis* transcript sequences expressed during infection reveals isolate-specific effectors. *PLoS One*, 6(5), e19328. <https://doi.org/10.1371/journal.pone.0019328>.
- Cai, M., Wang, Z., Ni, X., Hou, Y., Peng, Q., Gao, X., et al. (2019). Insights from the proteome profile of *Phytophthora capsici* in response to the novel fungicide SYP-14288. *PeerJ*, 7 e7626. <https://doi.org/10.7717/peerj.7626>.
- Capella-Gutierrez, S., Silla-Martinez, J. M., & Gabaldon, T. (2009). trimAl: A tool for automated alignment trimming in large-scale phylogenetic analyses. *Bioinformatics*, 25(15), 1972–1973. <https://doi.org/10.1093/bioinformatics/btp348>.

- Chen, X.-R., Xing, Y.-P., Li, Y.-P., Tong, Y.-H., & Xu, J.-Y. (2013). RNA-seq reveals infection-related gene expression changes in *Phytophthora capsici*. *PLoS One*, 8(9), e74588. <https://doi.org/10.1371/journal.pone.0074588>.
- Cheung, F., Win, J., Lang, J. M., Hamilton, J., Vuong, H., Leach, J. E., et al. (2008). Analysis of the *Pythium ultimum* transcriptome using Sanger and Pyrosequencing approaches. *BMC Genomics*, 9(1), 542. <https://doi.org/10.1186/1471-2164-9-542>.
- Cissé, O. H., & Stajich, J. E. (2019). FGMP: Assessing fungal genome completeness. *BMC Bioinformatics*, 20(1), 184. <https://doi.org/10.1186/s12859-019-2782-9>.
- Cui, C., Herlihy, J., Bombarely, A., McDowell, J. M., & Haak, D. C. (2019). Draft assembly of *Phytophthora capsici* from long-read sequencing uncovers complexity. *Molecular Plant-Microbe Interactions*, 10(1), 1559–1563. MPMI-04-19-0103-TA. <https://doi.org/10.1094/MPMI-04-19-0103-TA>.
- Dale, A. L., Feau, N., Everhart, S. E., Dhillon, B., Wong, B., Sheppard, J., et al. (2019). Mitotic recombination and rapid genome evolution in the invasive forest pathogen *Phytophthora ramorum*. *MBio*, 10(2), 1–19. <https://doi.org/10.1128/mBio.02452-18>.
- de Cock, A. W. A. M., Lodhi, A. M., Rintoul, T. L., Bala, K., Robideau, G. P., Abad, Z. G., et al. (2015). *Phytophthora*: Molecular phylogeny and systematics. *Persoonia*, 34(1), 25–39. <https://doi.org/10.3767/003158515X685382>.
- de Vries, S., de Vries, J., Archibald, J. M., & Slamovits, C. H. (2019). Comparative analyses of saprotrophy in *Salisaplia sapeloensis* and diverse plant pathogenic oomycetes reveal lifestyle-specific gene expression. *BioRxiv*, 656496. <https://doi.org/10.1101/656496>.
- Derevnina, L., Chin-Wo-Reyes, S., Martin, F., Wood, K., Froenicke, L., Spring, O., et al. (2015). Genome sequence and architecture of the tobacco downy mildew pathogen *Peronospora tabacina*. *Molecular Plant-Microbe Interactions*, 28(11), 1198–1215. <https://doi.org/10.1094/MPMI-05-15-0112-R>.
- Dong, S., Raffaele, S., & Kamoun, S. (2015). The two-speed genomes of filamentous pathogens: Waltz with plants. *Current Opinion in Genetics & Development*, 35, 57–65. <https://doi.org/10.1016/j.gde.2015.09.001>.
- Dou, D., Kale, S. D., Wang, X., Jiang, R. H. Y., Bruce, N. A., Arredondo, F. D., et al. Tyler, B. M., (2008). RXLR-mediated entry of *Phytophthora sojae* effector Avr1b into soybean cells does not require pathogen-encoded machinery. *The Plant Cell*, 20(7), 1930–1947. <https://doi.org/10.1105/tpc.107.056093>.
- Dussert, Y., Mazet, I. D., Couture, C., Gouzy, J., Piron, M.-C., Kuchly, C., et al. (2019). A high-quality grapevine downy mildew genome assembly reveals rapidly evolving and lineage-specific putative host adaptation genes. *Genome Biology and Evolution*, 11(3), 954–969. <https://doi.org/10.1093/gbe/evz048>.
- Edgar, R. C. (2004). MUSCLE: Multiple sequence alignment with high accuracy and high throughput. *Nucleic Acids Research*, 32(5), 1792–1797. <https://doi.org/10.1093/nar/gkh340>.
- Emms, D. M., & Kelly, S. (2019). OrthoFinder: Phylogenetic orthology inference for comparative genomics. *Genome Biology*, 20(1), 238. <https://doi.org/10.1186/s13059-019-1832-y>.
- Evangelisti, E., Gogleva, A., Hainaux, T., Doumane, M., Tulin, F., Quan, C., et al. (2017). Time-resolved dual transcriptomics reveal early induced *Nicotiana benthamiana* root genes and conserved infection-promoting *Phytophthora palmivora* effectors. *BMC Biology*, 15(1), 39. <https://doi.org/10.1186/s12915-017-0379-1>.
- Fang, Y., Coelho, M. A., Shu, H., Schotanus, K., Thimmappa, B. C., Yadav, V., et al. (2020). Long transposon-rich centromeres in an oomycete reveal divergence of centromere features in Stramenopila-Alveolata-Rhizaria lineages. *PLOS Genetics*, 16(3), e1008646. <https://doi.org/10.1371/journal.pgen.1008646>.
- Feau, N., Taylor, G., Dale, A. L., Dhillon, B., Bilodeau, G. J., Birol, I., et al. (2016). Genome sequences of six *Phytophthora* species threatening forest ecosystems. *Genomics Data*, 10, 85–88. <https://doi.org/10.1016/j.gdata.2016.09.013>.

- Finn, R. D., Attwood, T. K., Babbitt, P. C., Bateman, A., Bork, P., Bridge, A. J., et al. (2017). InterPro in 2017—Beyond protein family and domain annotations. *Nucleic Acids Research*, 45(D1), D190–D199. <https://doi.org/10.1093/nar/gkw1107>.
- Finn, R. D., Coggill, P., Eberhardt, R. Y., Eddy, S. R., Mistry, J., Mitchell, A. L., et al. (2016). The Pfam protein families database: Towards a more sustainable future. *Nucleic Acids Research*, 44(D1), D279–D285. <https://doi.org/10.1093/nar/gkv1344>.
- Fletcher, K., Gil, J., Bertier, L. D., Kenefick, A., Wood, K. J., Zhang, L., et al. (2019). Genomic signatures of heterokaryosis in the oomycete pathogen *Bremia lactucae*. *Nature Communications*, 10(1), 1–13. <https://doi.org/10.1038/s41467-019-10550-0>.
- Fletcher, K., Klosterman, S. J., Derevnina, L., Martin, F., Bertier, L. D., Koike, S., et al. (2018). Comparative genomics of downy mildews reveals potential adaptations to biotrophy. *BMC Genomics*, 19(1), 8–10. <https://doi.org/10.1186/s12864-018-5214-8>.
- Gaastera, W., Lipman, L. J. A., De Cock, A. W. A. M., Exel, T. K., Pegge, R. B. G., Scheurwater, J., et al. (2010). *Pythium insidiosum*: An overview. *Veterinary Microbiology*, 146(1–2), 1–16. <https://doi.org/10.1016/j.vetmic.2010.07.019>.
- Gao, R., Cheng, Y., Wang, Y., Wang, Y., Guo, L., & Zhang, G. (2015). Genome sequence of *Phytophthora fragariae* var. *fragariae*, a quarantine plant-pathogenic fungus. *Genome Announcements*, 3(2), 6–7. <https://doi.org/10.1128/genomeA.00034-15>.
- Gaulin, E., Pel, M. J. C., Camborde, L., San-Clemente, H., Courbier, S., Dupouy, M.-A., et al. (2018). Genomics analysis of *Aphanomyces* spp. identifies a new class of oomycete effector associated with host adaptation. *BMC Biology*, 16(1), 43. <https://doi.org/10.1186/s12915-018-0508-5>.
- Grayburn, W. S., Hudspeth, D. S. S., Gane, M. K., & Hudspeth, M. E. S. (2004). The mitochondrial genome of *Saprolegnia ferax*: Organization, gene content and nucleotide sequence. *Mycologia*, 96(5), 981–989. <https://doi.org/10.1080/15572536.2005.11832898>.
- Grenville-Briggs, L. J., Anderson, V. L., Fugelstad, J., Avrova, A. O., Bouzenzana, J., Williams, A., et al. (2008). Cellulose synthesis in *Phytophthora infestans* is required for normal appressorium formation and successful infection of potato. *The Plant Cell*, 20(3), 720–738. <https://doi.org/10.1105/tpc.107.052043>.
- Grenville-Briggs, L. J., Avrova, A. O., Hay, R. J., Bruce, C. R., Whisson, S. C., & van West, P. (2010). Identification of appressorial and mycelial cell wall proteins and a survey of the membrane proteome of *Phytophthora infestans*. *Fungal Biology*, 114(9), 702–723. <https://doi.org/10.1016/j.funbio.2010.06.003>.
- Grünwald, N. J., Martin, F. N., Larsen, M. M., Sullivan, C. M., Press, C. M., Coffey, M. D., et al. (2011). *Phytophthora-ID*.org: A sequence-based *Phytophthora* identification tool. *Plant Disease*, 95(3), 337–342. <https://doi.org/10.1094/PDIS-08-10-0609>.
- Haas, B. J., Kamoun, S., Zody, M. C., Jiang, R. H. Y., Handsaker, R. E., Cano, L. M., et al. (2009). Genome sequence and analysis of the Irish potato famine pathogen *Phytophthora infestans*. *Nature*, 461(7262), 393–398. <https://doi.org/10.1038/nature08358>.
- Hao, K., Lin, B., Nian, F., Gao, X., Wei, Z., Luo, G., et al. (2019). RNA-seq analysis of the response of plant-pathogenic oomycete *Phytophthora parasitica* to the fungicide dimethomorph. *Revista Argentina de Microbiología*, 51(3), 268–277. <https://doi.org/10.1016/j.ram.2018.08.007>.
- Hardham, A. R. (2005). *Phytophthora cinnamomi*. *Molecular Plant Pathology*, 6, 589–604. John Wiley & Sons, Ltd (10.1111). <https://doi.org/10.1111/j.1364-3703.2005.00308.x>.
- Horner, N. R., Grenville-Briggs, L. J., & van West, P. (2012). The oomycete *Pythium oligandrum* expresses putative effectors during mycoparasitism of *Phytophthora infestans* and is amenable to transformation. *Fungal Biology*, 116(1), 24–41. <https://doi.org/10.1016/j.funbio.2011.09.004>.
- Hosseini, S., Resjö, S., Liu, Y., Durling, M., Heyman, F., Levander, F., et al. (2015). Comparative proteomic analysis of hyphae and germinating cysts of *Phytophthora pisi* and *Phytophthora sojae*. *Journal of Proteomics*, 117, 24–40. <https://doi.org/10.1016/j.jpro.2015.01.006>.

- Hu, K., Ma, R.-R., Cheng, J.-M., Ye, X., Sun, Q., Yuan, H.-L., et al. (2016). Analysis of *Saprolegnia parasitica* transcriptome following treatment with copper sulfate. *PLoS One*, 11(2), e0147445. <https://doi.org/10.1371/journal.pone.0147445>.
- Jiang, R. H. Y., de Bruijn, I., Haas, B. J., Belmonte, R., Löbach, L., Christie, J., et al. (2013). Distinctive expansion of potential virulence genes in the genome of the oomycete fish pathogen *Saprolegnia parasitica*. *PLoS Genetics*, 9(6), e1003272. <https://doi.org/10.1371/journal.pgen.1003272>.
- Jiang, R. H. Y., Tyler, B. M., & Govers, F. (2006). Comparative analysis of phytophthora genes encoding secreted proteins reveals conserved synteny and lineage-specific gene duplications and deletions. *Molecular Plant-Microbe Interactions*, 19(12), 1311–1321. <https://doi.org/10.1094/MPMI-19-1311>.
- Jiang, R. H. Y., Tyler, B. M., Whisson, S. C., Hardham, A. R., & Govers, F. (2006). Ancient origin of elicitor gene clusters in Phytophthora genomes. *Molecular Biology and Evolution*, 23(2), 338–351. <https://doi.org/10.1093/molbev/msj039>.
- Judelson, H. S., Shrivastava, J., & Manson, J. (2012). Decay of genes encoding the oomycete flagellar proteome in the downy mildew *Hyaloperonospora arabidopsidis*. *PLoS One*, 7(10), e47624. <https://doi.org/10.1371/journal.pone.0047624>.
- Jupe, J., Stam, R., Howden, A. J. M., Morris, J. A., Zhang, R., Hedley, P. E., et al. (2013). Phytophthora capsici-tomato interaction features dramatic shifts in gene expression associated with a hemi-biotrophic lifestyle. *Genome Biology*, 14(6), R63. <https://doi.org/10.1186/gb-2013-14-6-r63>.
- Kalyanamoorthy, S., Minh, B. Q., Wong, T. K. F., von Haeseler, A., & Jermini, L. S. (2017). ModelFinder: Fast model selection for accurate phylogenetic estimates. *Nature Methods*, 14(6), 587–589. <https://doi.org/10.1038/nmeth.4285>.
- Kamoun, S. (2003). Molecular genetics of pathogenic oomycetes. *Eukaryotic Cell*, 2(2), 191–199. <https://doi.org/10.1128/ec.2.2.191-199.2003>.
- Kamoun, S. (2006). A catalogue of the effector secretome of plant pathogenic oomycetes. *Annual Review of Phytopathology*, 44, 41–60. <https://doi.org/10.1146/annurev.phyto.44.070505.143436>.
- Kemen, E., Gardiner, A., Schultz-Larsen, T., Kemen, A. C., Balmuth, A. L., Robert-Seilantian, A., et al. (2011). Gene gain and loss during evolution of obligate parasitism in the white rust pathogen of *Arabidopsis thaliana*. *PLoS Biology*, 9(7), e1001094. <https://doi.org/10.1371/journal.pbio.1001094>.
- Krings, M., Taylor, T. N., & Dotzler, N. (2011). The fossil record of the Peronosporomycetes (Oomycota). *Mycologia*, 103(3), 445–457. <https://doi.org/10.3852/10-278>.
- Krogh, A., Larsson, B., von Heijne, G., & Sonnhammer, E. L. (2001). Predicting transmembrane protein topology with a hidden Markov model: Application to complete genomes. *Journal of Molecular Biology*, 305(3), 567–580. <https://doi.org/10.1006/jmbi.2000.4315>.
- Kushwaha, S. K., Vetukuri, R. R., & Grenville-Briggs, L. J. (2017a). Draft genome sequence of the mycoparasitic oomycete *Pythium oligandrum* strain CBS 530.74. *Genome Announcements*, 5(21), e00556–18. <https://doi.org/10.1128/genomeA.00346-17>.
- Kushwaha, S. K., Vetukuri, R. R., & Grenville-Briggs, L. J. (2017b). Draft genome sequence of the mycoparasitic oomycete *Pythium periplocum* strain CBS 532.74. *Genome Announcements*, 5(12), e00556–18. <https://doi.org/10.1128/genomeA.00057-17>.
- Lamour, K. H., Mudge, J., Gobena, D., Hurtado-Gonzales, O. P., Schmutz, J., Kuo, A., et al. (2012). Genome sequencing and mapping reveal loss of heterozygosity as a mechanism for rapid adaptation in the vegetable pathogen *Phytophthora capsici*. *Molecular Plant-Microbe Interactions*, 25(10), 1350–1360. <https://doi.org/10.1094/MPMI-02-12-0028-R>.
- Lassiter, E. S., Russ, C., Nusbaum, C., Zeng, Q., Saville, A. C., Olarte, R. A., et al. (2015). Mitochondrial genome sequences reveal evolutionary relationships of the *Phytophthora* 1c clade species. *Current Genetics*, 61(4), 567–577. <https://doi.org/10.1007/s00294-015-0480-3e>.

- Lee, S.-J., Kelley, B. S., Damasceno, C. M. B., John, B. S., Kim, B.-S., Kim, B.-D., et al. (2006). A functional screen to characterize the secretomes of eukaryotic pathogens and their hosts in planta. *Molecular Plant-Microbe Interactions*, 19(12), 1368–1377. <https://doi.org/10.1094/MPMI-19-1368>.
- Leonard, G., Labarre, A., Milner, D. S., Monier, A., Soanes, D., Wideman, J. G., et al. (2018). Comparative genomic analysis of the ‘pseudofungus’ *Hyphochytrium catenoides*. *Open Biology*, 8(1), 170184. <https://doi.org/10.1098/rsob.170184>.
- Letunic, I., & Bork, P. (2007). Interactive Tree Of Life (iTOL): An online tool for phylogenetic tree display and annotation. *Bioinformatics*, 23(1), 127–128. <https://doi.org/10.1093/bioinformatics/btl529>.
- Lévesque, C. A., Brouwer, H., Cano, L., Hamilton, J. P., Holt, C., Huitema, E., et al. (2010). Genome sequence of the necrotrophic plant pathogen *Pythium ultimum* reveals original pathogenicity mechanisms and effector repertoire. *Genome Biology*, 11(7), R73. <https://doi.org/10.1186/gb-2010-11-7-r73>.
- Lévesque, C. A., & De Cock, A. W. A. M. (2004). Molecular phylogeny and taxonomy of the genus *Pythium*. *Mycological Research*, 108(12), 1363–1383. <https://doi.org/10.1017/S0953756204001431>.
- Links, M. G., Holub, E., Jiang, R. H., Sharpe, A. G., Hegedus, D., Beynon, E., et al. (2011). De novo sequence assembly of *Albugo candida* reveals a small genome relative to other biotrophic oomycetes. *BMC Genomics*, 12(1), 503. <https://doi.org/10.1186/1471-2164-12-503>.
- Liu, H., Ma, X., Yu, H., Fang, D., Li, Y., Wang, X., et al. (2016). Genomes and virulence difference between two physiological races of *Phytophthora nicotianae*. *GigaScience*, 5(1), 3. <https://doi.org/10.1186/s13742-016-0108-7>.
- Malar, C. M., Yuzon, J. D., Das, S., Das, A., Panda, A., Ghosh, S., et al. (2019). Haplotype-phased genome assembly of virulent *Phytophthora ramorum* isolate ND886 facilitated by long-read sequencing reveals effector polymorphisms and copy number variation. *Molecular Plant-Microbe Interactions*, 32(8), 1047–1060. <https://doi.org/10.1094/MPMI-08-18-0222-R>.
- Malar, C. M., Yuzon, J. D., Panda, A., Kasuga, T., & Tripathy, S. (2019). Updated assembly resource of *Phytophthora ramorum* Pr102 isolate incorporating long reads from PacBio sequencing. *Molecular Plant-Microbe Interactions*, 32, 1472–1474. <https://doi.org/10.1094/MPMI-05-19-0147-A>.
- Martin, F. N., Bensasson, D., Tyler, B. M., & Boore, J. L. (2007). Mitochondrial genome sequences and comparative genomics of *Phytophthora ramorum* and *P. sojae*. *Current Genetics*, 51(5), 285–296. <https://doi.org/10.1007/s00294-007-0121-6>.
- Martin, F. N., Blair, J. E., & Coffey, M. D. (2014). A combined mitochondrial and nuclear multilocus phylogeny of the genus *Phytophthora*. *Fungal Genetics and Biology*, 66, 19–32. <https://doi.org/10.1016/j.fgb.2014.02.006>.
- Matari, N. H., & Blair, J. E. (2014). A multilocus timescale for oomycete evolution estimated under three distinct molecular clock models. *BMC Evolutionary Biology*, 14(1), 101. <https://doi.org/10.1186/1471-2148-14-101>.
- McCarthy, C. G. P., & Fitzpatrick, D. A. (2016). Systematic search for evidence of inter-domain horizontal gene transfer from prokaryotes to oomycete lineages. *MSphere*, 1(5), 1–18. <https://doi.org/10.1128/mSphere.00195-16>.
- McCarthy, C. G. P., & Fitzpatrick, D. A. (2017). Phylogenomic reconstruction of the oomycete phylogeny derived from 37 genomes. *MSphere*, 2(2), e00095-17. <https://doi.org/10.1128/mSphere.00095-17>.
- McGowan, J., Byrne, K. P., & Fitzpatrick, D. A. (2019). Comparative analysis of oomycete genome evolution using the oomycete gene order browser (GOB). *Genome Biology and Evolution*, 11(1), 189–206. <https://doi.org/10.1093/gbe/evy267>.
- McGowan, J., & Fitzpatrick, D. A. (2017). Genomic, network, and phylogenetic analysis of the oomycete effector arsenal. *MSphere*, 2(6), e00408–e00417. <https://doi.org/10.1128/mSphere.00408-17>.

- Meijer, H. J. G., Mancuso, F. M., Espadas, G., Seidl, M. F., Chiva, C., Govers, F., et al. (2014). Profiling the secretome and extracellular proteome of the potato late blight pathogen *Phytophthora infestans*. *Molecular & Cellular Proteomics*, 13(8), 2101–2113. <https://doi.org/10.1074/mcp.M113.035873>.
- Misner, I., Blouin, N., Leonard, G., Richards, T. A., & Lane, C. E. (2015). The secreted proteins of *Achlya hypogyna* and *Thraustotheca clavata* identify the ancestral oomycete secretome and reveal gene acquisitions by horizontal gene transfer. *Genome Biology and Evolution*, 7(1), 120–135. <https://doi.org/10.1093/gbe/evu276>.
- Nayaka, S. C., Shetty, H. S., Satyavathi, C. T., Yadav, R. S., Kishor, P. B. K., Nagaraju, M., et al. (2017). Draft genome sequence of *Sclerospora graminicola*, the pearl millet downy mildew pathogen. *Biotechnology Reports*, 16(August), 18–20. <https://doi.org/10.1016/j.btre.2017.07.006>.
- Nguyen, L. T., Schmidt, H. A., Von Haeseler, A., & Minh, B. Q. (2015). IQ-TREE: A fast and effective stochastic algorithm for estimating maximum-likelihood phylogenies. *Molecular Biology and Evolution*, 32(1), 268–274. <https://doi.org/10.1093/molbev/msu300>.
- Oome, S., Raaymakers, T. M., Cabral, A., Samwel, S., Böhm, H., Albert, I., et al. (2014). Nep1-like proteins from three kingdoms of life act as a microbe-associated molecular pattern in *Arabidopsis*. *Proceedings of the National Academy of Sciences of the United States of America*, 111(47), 16955–16960. <https://doi.org/10.1073/pnas.1410031111>.
- Orsomando, G., Lorenzi, M., Raffaelli, N., Dalla Rizza, M., Mezzetti, B., & Ruggieri, S. (2001). Phytotoxic protein PcF, purification, characterization, and cDNA sequencing of a novel hydroxyproline-containing factor secreted by the strawberry pathogen *Phytophthora cactorum*. *Journal of Biological Chemistry*, 276(24), 21578–21584. <https://doi.org/10.1074/jbc.M101377200>.
- Panda, A., Sen, D., Ghosh, A., Gupta, A., Mathu Malar, C., Prakash Mishra, G., et al. (2018). EumicrobeDBLite: A lightweight genomic resource and analytic platform for draft oomycete genomes. *Molecular Plant Pathology*, 19(1), 227–237. <https://doi.org/10.1111/mps.12505>.
- Paquin, B., Laforest, M.-J., Forget, L., Roewer, I., Wang, Z., Longcore, J., et al. (1997). The fungal mitochondrial genome project: Evolution of fungal mitochondrial genomes and their gene expression. *Current Genetics*, 31(5), 380–395. <https://doi.org/10.1007/s002940050220>.
- Raaymakers, T. M., & Van den Ackerveken, G. (2016). Extracellular recognition of oomycetes during biotrophic infection of plants. *Frontiers in Plant Science*, 7(June), 1–12. <https://doi.org/10.3389/fpls.2016.00906>.
- Raffaele, S., Win, J., Cano, L. M., & Kamoun, S. (2010). Analyses of genome architecture and gene expression reveal novel candidate virulence factors in the secretome of *Phytophthora infestans*. *BMC Genomics*, 11(1), 637. <https://doi.org/10.1186/1471-2164-11-637>.
- Rahman, A., Góngora-Castillo, E., Bowman, M. J., Childs, K. L., Gent, D. H., Martin, F. N., et al. (2019). Genome sequencing and transcriptome analysis of the hop downy mildew pathogen *Pseudoperonospora humuli* reveal species-specific genes for molecular detection. *Phytopathology*, 109(8), 1354–1366. <https://doi.org/10.1094/PHYTO-11-18-0431-R>.
- Resjö, S., Ali, A., Meijer, H. J. G., Seidl, M. F., Snel, B., Sandin, M., et al. (2014). Quantitative label-free phosphoproteomics of six different life stages of the late blight pathogen *Phytophthora infestans* reveals abundant phosphorylation of members of the CRN effector family. *Journal of Proteome Research*, 13(4), 1848–1859. <https://doi.org/10.1021/pr4009095>.
- Resjö, S., Brus, M., Ali, A., Meijer, H. J. G., Sandin, M., Govers, F., et al. (2017). Proteomic analysis of *Phytophthora infestans* reveals the importance of cell wall proteins in pathogenicity. *Molecular & Cellular Proteomics*, 16(11), 1958–1971. <https://doi.org/10.1074/mcp.M116.065656>.

- Rhoads, A., & Au, K. F. (2015). PacBio sequencing and its applications. *Genomics, Proteomics & Bioinformatics*, 13(5), 278–289. <https://doi.org/10.1016/j.gpb.2015.08.002>.
- Richards, T. A., Dacks, J. B., Jenkinson, J. M., Thornton, C. R., & Talbot, N. J. (2006). Evolution of filamentous plant pathogens: Gene exchange across eukaryotic kingdoms. *Current Biology*, 16(18), 1857–1864. <https://doi.org/10.1016/j.cub.2006.07.052>.
- Richards, T. A., Soanes, D. M., Jones, M. D. M., Vasieva, O., Leonard, G., Paszkiewicz, K., et al. (2011). Horizontal gene transfer facilitated the evolution of plant parasitic mechanisms in the oomycetes. *Proceedings of the National Academy of Sciences of the United States of America*, 108(37), 15258–15263. <https://doi.org/10.1073/pnas.1105100108>.
- Rizzo, D. M., Garbelotto, M., & Hansen, E. M. (2005). Phytophthora ramorum: Integrative research and management of an emerging pathogen in California and Oregon forests. *Annual Review of Phytopathology*, 43(1), 309–335. <https://doi.org/10.1146/annurev.phyto.42.040803.140418>.
- Roquigny, R., Novinscak, A., Arseneault, T., Joly, D. L., & Fillion, M. (2018). Transcriptome alteration in Phytophthora infestans in response to phenazine-1-carboxylic acid production by Pseudomonas fluorescens strain LBUM223. *BMC Genomics*, 19(1), 474. <https://doi.org/10.1186/s12864-018-4852-1>.
- Rujirawat, T., Patumcharoenpol, P., Lohnoo, T., Yingyong, W., Kumsang, Y., Payattikul, P., et al. (2018). Probing the phylogenomics and putative pathogenicity genes of Pythium insidiosum by oomycete genome analyses. *Scientific Reports*, 8(1), 4135. <https://doi.org/10.1038/s41598-018-22540-1>.
- Rujirawat, T., Patumcharoenpol, P., Lohnoo, T., Yingyong, W., Leksuthirath, T., Tangphatsornruang, S., et al. (2015). Draft genome sequence of the pathogenic oomycete Pythium insidiosum strain Pi-S, isolated from a patient with pythiosis. *Genome Announcements*, 3(3), e00574–15. <https://doi.org/10.1128/genomeA.00574-15>.
- Savidor, A., Donahoo, R. S., Hurtado-Gonzales, O., Land, M. L., Shah, M. B., Lamour, K. H., et al. (2008). Cross-species global proteomics reveals conserved and unique processes in Phytophthora sojae and Phytophthora ramorum. *Molecular & Cellular Proteomics*, 7(8), 1501–1516. <https://doi.org/10.1074/mcp.M700431-MCP200>.
- Savory, F. R., Leonard, G., & Richards, T. A. (2015). The role of horizontal gene transfer in the evolution of the oomycetes. *PLoS Pathogens*, 11(5), e1004805. <https://doi.org/10.1371/journal.ppat.1004805>.
- Savory, F. R., Milner, D. S., Miles, D. C., & Richards, T. A. (2018). Ancestral function and diversification of a horizontally acquired oomycete carboxylic acid transporter. *Molecular Biology and Evolution*, 35(8), 1887–1900. <https://doi.org/10.1093/molbev/msy082>.
- Schornack, S., van Damme, M., Bozkurt, T. O., Cano, L. M., Smoker, M., Thines, M., et al. (2010). Ancient class of translocated oomycete effectors targets the host nucleus. *Proceedings of the National Academy of Sciences of the United States of America*, 107(40), 17421–17426. <https://doi.org/10.1073/pnas.1008491107>.
- Seidl, M. F., & Van den Ackerveken, G. (2019). Activity and phylogenetics of the broadly occurring family of microbial Nep1-like proteins. *Annual Review of Phytopathology*, 57(1), 367–386. <https://doi.org/10.1146/annurev-phyto-082718-100054>.
- Seidl, M. F., Van Den Ackerveken, G., Govers, F., & Snel, B. (2012). Reconstruction of oomycete genome evolution identifies differences in evolutionary trajectories leading to present-day large gene families. *Genome Biology and Evolution*, 4(3), 199–211. <https://doi.org/10.1093/gbe/evs003>.
- Severino, V., Farina, A., Fleischmann, F., Dalio, R. J. D., Di Maro, A., Scognamiglio, M., et al. (2014). Molecular profiling of the Phytophthora plurivora secretome: A step towards understanding the cross-talk between plant pathogenic oomycetes and their hosts. *PLoS One*, 9(11), e112317. <https://doi.org/10.1371/journal.pone.0112317>.

- Sharma, R., Xia, X., Cano, L. M., Evangelisti, E., Kemen, E., Judelson, H., et al. (2015). Genome analyses of the sunflower pathogen *Plasmopara halstedii* provide insights into effector evolution in downy mildews and *Phytophthora*. *BMC Genomics*, 16(1), 741. <https://doi.org/10.1186/s12864-015-1904-7>.
- Shen, D., Tang, Z., Wang, C., Wang, J., Dong, Y., Chen, Y., et al. (2019). Infection mechanisms and putative effector repertoire of the mosquito pathogenic oomycete *Pythium guiyangense* uncovered by genomic analysis. *PLoS Genetics*, 15(4), 1–26. <https://doi.org/10.1371/journal.pgen.1008116>.
- Sperschneider, J., Dodds, P. N., Gardiner, D. M., Manners, J. M., Singh, K. B., & Taylor, J. M. (2015). Advances and challenges in computational prediction of effectors from plant pathogenic fungi. *PLoS Pathogens*, 11(5), e1004806. <https://doi.org/10.1371/journal.ppat.1004806>.
- Sperschneider, J., Dodds, P. N., Gardiner, D. M., Singh, K. B., & Taylor, J. M. (2018). Improved prediction of fungal effector proteins from secretomes with EffectorP 2.0. *Molecular Plant Pathology*, 19(9), 2094–2110. <https://doi.org/10.1111/mpp.12682>.
- Sperschneider, J., Dodds, P. N., Singh, K. B., & Taylor, J. M. (2018). ApoplastP: Prediction of effectors and plant proteins in the apoplast using machine learning. *New Phytologist*, 217(4), 1764–1778. <https://doi.org/10.1111/nph.14946>.
- Spies, C. F. J., Grooters, A. M., Lévesque, C. A., Rintoul, T. L., Redhead, S. A., Glockling, S. L., et al. (2016). Molecular phylogeny and taxonomy of Lagenidium-like oomycetes pathogenic to mammals. *Fungal Biology*, 120(8), 931–947. <https://doi.org/10.1016/j.funbio.2016.05.005>.
- Srivastava, V., Rezinciuc, S., & Bulone, V. (2018). Quantitative proteomic analysis of four developmental stages of *Saprolegnia parasitica*. *Frontiers in Microbiology*, 8(Jan), 1–13. <https://doi.org/10.3389/fmicb.2017.02658>.
- Studholme, D. J., McDougal, R. L., Sambles, C., Hansen, E., Hardy, G., Grant, M., et al. (2015). Genome sequences of six *Phytophthora* species associated with forests in New Zealand. *Genomics Data*, 7, 54–56. <https://doi.org/10.1016/j.gdata.2015.11.015>.
- Studholme, D. J., Panda, P., Sanfuentes Von Stowasser, E., González, M., Hill, R., Sambles, C., et al. (2019). Genome sequencing of oomycete isolates from Chile supports the New Zealand origin of *Phytophthora kernoviae* and makes available the first *Nothophytophthora* sp. genome. *Molecular Plant Pathology*, 20(3), 423–431. <https://doi.org/10.1111/mpp.12765>.
- Sun, J., Gao, Z., Zhang, X., Zou, X., Cao, L., & Wang, J. (2017). Transcriptome analysis of *Phytophthora litchii* reveals pathogenicity arsenals and confirms taxonomic status. *PLoS One*, 12(6) e0178245. <https://doi.org/10.1371/journal.pone.0178245>.
- Tabima, J. F., Kronmiller, B. A., Press, C. M., Tyler, B. M., Zasada, I. A., & Grünwald, N. J. (2017). Whole genome sequences of the Raspberry and Strawberry pathogens *Phytophthora rubi* and *P. fragariae*. *Molecular Plant-Microbe Interactions*, 30(10), 767–769. <https://doi.org/10.1094/MPMI-04-17-0081-A>.
- Tangphatsornruang, S., Ruang-areerate, P., Sangrakru, D., Rujirawat, T., Lohnoo, T., Kittichotirat, W., et al. (2016). Comparative mitochondrial genome analysis of *Pythium insidiosum* and related oomycete species provides new insights into genetic variation and phylogenetic relationships. *Gene*, 575(1), 34–41. <https://doi.org/10.1016/j.gene.2015.08.036>.
- Thines, M., & Kamoun, S. (2010). Oomycete–plant coevolution: Recent advances and future prospects. *Current Opinion in Plant Biology*, 13(4), 427–433. <https://doi.org/10.1016/j.pbi.2010.04.001>.
- Thines, M., Sharma, R., Rodenburg, S. Y. A., Gogleva, A., Judelson, H. S., Xia, X., et al. (2019). The genome of *Peronospora belbahrii* reveals high heterozygosity, a low number of canonical effectors and CT-rich promoters. *BioRxiv*, 721027. <https://doi.org/10.1101/721027>.

- Tian, M., Win, J., Song, J., van der Hoorn, R., van der Knaap, E., & Kamoun, S. (2006). A *Phytophthora infestans* cystatin-like protein targets a novel tomato papain-like apoplastic protease. *Plant Physiology*, 143(1), 364–377. <https://doi.org/10.1104/pp.106.090050>.
- Torto, T., Rauser, L., & Kamoun, S. (2002). The *pipg1* gene of the oomycete *Phytophthora infestans* encodes a fungal-like endopolygalacturonase. *Current Genetics*, 40(6), 385–390. <https://doi.org/10.1007/s00294-002-0272-4>.
- Tyler, B. M. (2007). *Phytophthora sojae*: Root rot pathogen of soybean and model oomycete. *Molecular Plant Pathology*, 8(1), 1–8. <https://doi.org/10.1111/j.1364-3703.2006.00373.x>.
- Tyler, B. M., Tripathy, S., Zhang, X., Dehal, P., Jiang, R. H. Y., Aerts, A., et al. (2006). *Phytophthora* genome sequences uncover evolutionary origins and mechanisms of pathogenesis. *Science (New York, N.Y.)*, 313(5791), 1261–1266. <https://doi.org/10.1126/science.1128796>.
- Urban, M., Cuzick, A., Rutherford, K., Irvine, A., Pedro, H., Pant, R., et al. (2017). PHI-base: A new interface and further additions for the multi-species pathogen–host interactions database. *Nucleic Acids Research*, 45(D1), D604–D610. <https://doi.org/10.1093/nar/gkw1089>.
- Uzuhashi, S., Endoh, R., Manabe, R., & Ohkuma, M. (2017). Draft genome sequences of the oomycete *Pilasporangium apinafurcum* strains JCM 30513 and JCM 30514, formerly classified as *Pythium apinafurcum*. *Genome Announcements*, 5(35), 4–5. <https://doi.org/10.1128/genomeA.00899-17>.
- van den Berg, A. H., McLaggan, D., Diéguez-Uribeondo, J., & van West, P. (2013). The impact of the water moulds *Saprolegnia diclina* and *Saprolegnia parasitica* on natural ecosystems and the aquaculture industry. *Fungal Biology Reviews*, 27(2), 33–42. <https://doi.org/10.1016/j.fbr.2013.05.001>.
- Vetukuri, R. R., Kushwaha, S. K., Sen, D., Whisson, S. C., Lamour, K. H., & Grenville-Briggs, L. J. (2018). Genome sequence resource for the oomycete taro pathogen *Phytophthora colocasiae*. *Molecular Plant-Microbe Interactions*, 31(9), 903–905. <https://doi.org/10.1094/MPMI-12-17-0321-A>.
- Vetukuri, R. R., Tripathy, S., Mathu, M. C., Panda, A., Kushwaha, S. K., Chawade, A., et al. (2018). Draft genome sequence for the tree pathogen *Phytophthora plurivora*. *Genome Biology and Evolution*, 10(9), 2432–2442. <https://doi.org/10.1093/gbe/evy162>.
- Vilela, R., Humber, R. A., Taylor, J. W., & Mendoza, L. (2019). Phylogenetic and physiological traits of oomycetes originally identified as *Lagenidium giganteum* from fly and mosquito larvae. *Mycologia*, 111(3), 408–422. <https://doi.org/10.1080/00275514.2019.1589316>.
- Wang, S., Boevink, P. C., Welsh, L., Zhang, R., Whisson, S. C., & Birch, P. R. J. (2017). Delivery of cytoplasmic and apoplastic effectors from *Phytophthora infestans* haustoria by distinct secretion pathways. *New Phytologist*, 216, 205–215. <https://doi.org/10.1111/nph.14696>.
- Wang, S., McLellan, H., Bukharova, T., He, Q., Murphy, F., Shi, J., et al. (2019). *Phytophthora infestans* RXLR effectors act in concert at diverse subcellular locations to enhance host colonization. *Journal of Experimental Botany*, 70(1), 343–356. <https://doi.org/10.1093/jxb/ery360>.
- Wang, S., Welsh, L., Thorpe, P., Whisson, S. C., Boevink, P. C., & Birch, P. R. J. (2018). The *Phytophthora infestans* haustorium is a site for secretion of diverse classes of infection-associated proteins. *MBio*, 9(4), 1–14. <https://doi.org/10.1128/mBio.01216-18>.
- Waterhouse, R. M., Seppey, M., Simão, F. A., Manni, M., Ioannidis, P., Klioutchnikov, G., et al. (2018). BUSCO applications from quality assessments to gene prediction and phylogenomics. *Molecular Biology and Evolution*, 35(3), 543–548. <https://doi.org/10.1093/molbev/msx319>.

- Wawra, S., Belmonte, R., Löbach, L., Saraiva, M., Willems, A., & van West, P. (2012). Secretion, delivery and function of oomycete effector proteins. *Current Opinion in Microbiology*, 15(6), 685–691. <https://doi.org/10.1016/j.mib.2012.10.008>.
- Whisson, S. C., Boevink, P. C., Moleleki, L., Avrova, A. O., Morales, J. G., Gilroy, E. M., et al. (2007). A translocation signal for delivery of oomycete effector proteins into host plant cells. *Nature*, 450(November), 115–118. <https://doi.org/10.1038/nature06203>.
- Whitaker, J. W., McConkey, G. A., & Westhead, D. R. (2009). The transferome of metabolic genes explored: Analysis of the horizontal transfer of enzyme encoding genes in unicellular eukaryotes. *Genome Biology*, 10(4), R36. <https://doi.org/10.1186/gb-2009-10-4-r36>.
- Win, J., Krasileva, K. V., Kamoun, S., Shirasu, K., Staskawicz, B. J., & Banfield, M. J. (2012). Sequence divergent RXLR effectors share a structural fold conserved across plant pathogenic oomycete species. *PLoS Pathogens*, 8(1), e1002400. <https://doi.org/10.1371/journal.ppat.1002400>.
- Yang, X., & Hong, C. (2018). Differential usefulness of nine commonly used genetic markers for identifying *Phytophthora* species. *Frontiers in Microbiology*, 9, 2334. <https://doi.org/10.3389/fmicb.2018.02334>.
- Ye, W., Wang, Y., Shen, D., Li, D., Pu, T., Jiang, Z., et al. (2016). Sequencing of the litchi downy blight pathogen reveals it is a *Phytophthora* species with downy mildew-like characteristics. *Molecular Plant-Microbe Interactions*, 29(7), 573–583. <https://doi.org/10.1094/MPMI-03-16-0056-R>.
- Yin, L., An, Y., Qu, J., Li, X., Zhang, Y., Dry, I., et al. (2017). Genome sequence of *Plasmopara viticola* and insight into the pathogenic mechanism. *Scientific Reports*, 7, 46553. <https://doi.org/10.1038/srep46553>.
- Yin, J., Gu, B., Huang, G., Tian, Y., Quan, J., Lindqvist-Kreuzer, H., et al. (2017). Conserved RXLR effector genes of *Phytophthora infestans* expressed at the early stage of potato infection are suppressive to host defense. *Frontiers in Plant Science*, 8, 1–11. <https://doi.org/10.3389/fpls.2017.02155>.
- Yuan, X., Feng, C., Zhang, Z., & Zhang, C. (2017). Complete mitochondrial genome of *Phytophthora nicotianae* and identification of molecular markers for the oomycetes. *Frontiers in Microbiology*, 8, 1–14. <https://doi.org/10.3389/fmicb.2017.01484>.
- Zerillo, M. M., Adhikari, B. N., Hamilton, J. P., Buell, C. R., Lévesque, C. A., & Tisserat, N. (2013). Carbohydrate-active enzymes in *pythium* and their role in plant cell wall and storage polysaccharide degradation. *PLoS One*, 8(9), e72572. <https://doi.org/10.1371/journal.pone.0072572>.
- Zheng, X., McLellan, H., Fraiture, M., Liu, X., Boevink, P. C., Gilroy, E. M., et al. (2014). Functionally redundant RXLR effectors from *Phytophthora infestans* act at different steps to suppress early flg22-triggered immunity. *PLoS Pathogens*, 10(4), e1004057. <https://doi.org/10.1371/journal.ppat.1004057>.